UNIVERSITY OF COLORADO - BOULDER

ASEN 4018

SENIOR PROJECTS II: DESIGN PRACTICUM | SPRING 2021

Balloon Deployment System
Project Final Report

Authors:

Aufa AMIRULLAH - 105272937

Peter HURST - 106038543

Matthew KONNATH - 105976578

Jake MCGRATH - 108497764

Grant NORMAN - 107478513

Patrick PALUSZEK - 106967379

Jack SOLTYS - 107565276

Kyler STIREWALT - 107283105

Sebastian URRUNAGA - 108269497

Chenshuo YANG - 107159043

Instructor:
Professor Jelliffe JACKSON

Advisor:
Matt RHODE

Customer:
Professor Dale LAWRENCE

May 3, 2021

College of Engineering & Applied Science
UNIVERSITY OF COLORADO BOULDER

Contents

List of Figures

Acronyms

AFOSR Air Force Office of Scientific Research

BDS Balloon Deployment System

CDR Critical Design Review

CONOPS Concept of Operations

FOS Factor of Safety

FR Functional Requirement

HYFLITS Hypersonic Flight in the Turbulent Stratosphere

IO Initially Open

MIMO Multiple Input Multiple Output

OSHA Occupational Safety and Health Administration

PDR Preliminary Design Review

PFR Project Final Review

RF Radio Frequency

SISO Single Input Single Output

Nomenclature

$\ddot{x}$	Acceleration of Balloon [m/s^2]
$\dot{x}$	Velocity of Balloon [m/s]
μ	Coefficient of Friction
ρ	Nominal Air Density [kg/m^3]
σ	Tensile Stress [Pa]
τ	Shear Stress [Pa]
A	Area [m^2]
a	Acceleration [m/s^2]
C_D	Balloon Drag Coefficient
D	Drag [N]
F	Force [N]
I	Current [A]
k	Balloon Neck System Equivalent Linear Stiffness [N/m]
M	Moment [N-m]
m	Mass [kg]
S	Balloon Characteristic Area
t	Time [s]
V	Voltage [V]
v	Velocity [m/s]
$w(t)$	Wind Speed [m/s]
$x(t)$	Position of Balloon [m]

I. Project Purpose

Authors: Jack Soltys

Presently the knowledge of turbulent patterns present at high altitudes is still limited, as current measurement methods are costly and ineffective. Last year, the Air Force Office of Scientific Research (AFOSR) funded a project named Hypersonic Flight in the Turbulent Stratosphere (HYFLITS) to collect turbulence data in this particular part of the atmosphere. Data collected will be used to develop high altitude aircraft operating in the stratosphere. In order to measure and collect the turbulence data, HYFLITS utilizes a weather balloon in the 20-40 km altitude range of interest. The Balloon Deployment System (BDS) aims to create a support system to aid in high wind, single person high altitude balloon launches.

Figure 1 Example of a typical balloon used during a launch

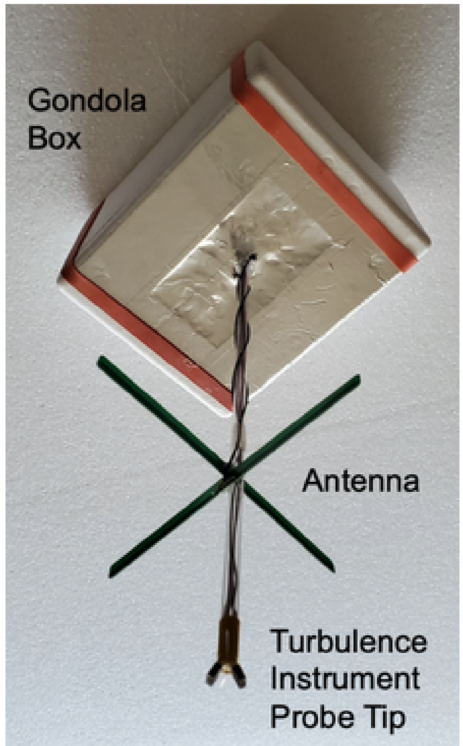

Figure 2 HYFLITS payload. Note the antenna extending out of the bottom of the payload

The current process of deploying these balloons with one individual poses a risk of damaging the data gathering payload and balloon in windy conditions. This process can be seen in Figure 1. With unpredictable weather conditions, it is imperative to set up and deploy the balloon in a streamlined manner and avoid damage to the delicate data acquisition payload, shown in Figure 2. The current deployment procedure is heavily limited by human reaction time, height, and difficulty associated with judging when a lull in the wind will occur, negatively impacting the safety and reliability of launch.

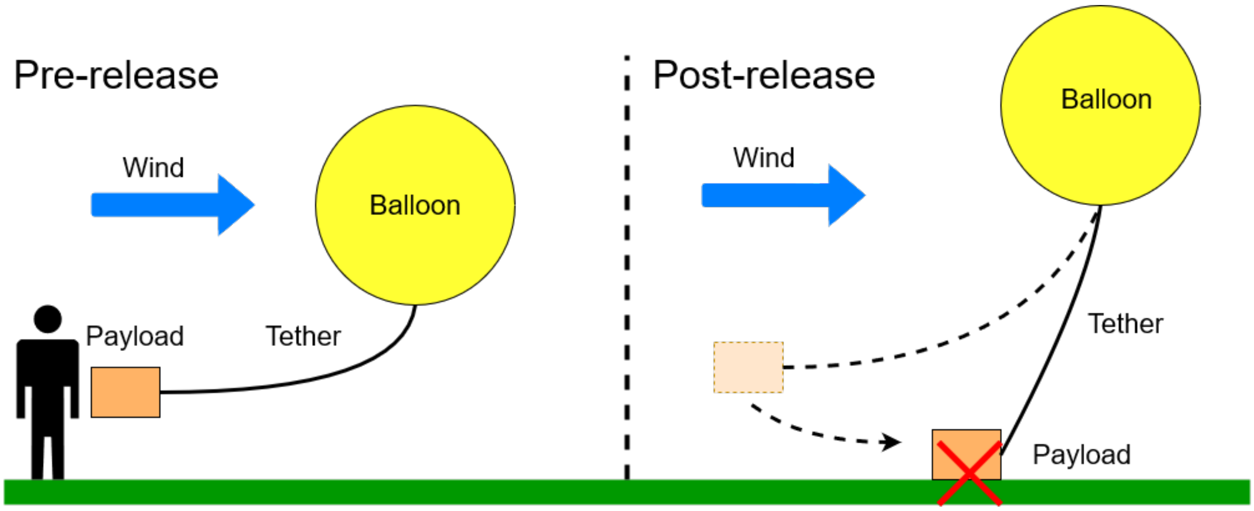

Figure 3 Illustration of the current deployment problem, showing risk of damage to the payload

Figure 3 further illustrates the risk of damage posed to the payload using current single user deployment methods. The current method involves the individual holding both the payload and the balloon simultaneously. Then, when a suitable time for the launch occurs (typically a lull in the wind), the individual releases the balloon while holding onto the payload until the balloon has lifted to a suitable height. At that point, once the balloon is at the desired height or distance away, the individual releases the payload. However, if the balloon is not at a sufficient altitude, the payload may swing into the ground, damaging the sensitive antenna shown in Figure 2. Managing the balloon, payload, and tether all in a high wind environment as well as ensuring that the payload is not damaged during launch are not trivial tasks. The BDS solves this issue by allowing the user to set up the system and balloon upwind of the payload, giving significantly more time for the balloon to gain height.

II. Project Objectives and Functional Requirements

Authors: Kyler Stirewalt, Jack Soltys, Sebastian Urrunaga

A. Level of Success

In order to achieve the minimum requirements of success for the BDS project, the launch system must be able to safely and reliably launch a balloon from a 3 m height in strong winds via user commands while being easy to assemble and transport by a single person. The structure of the balloon launcher shall be light and small enough to be transported in a 1m x 0.25 m cylindrical bag and easy yet intuitive to assemble and disassemble. Once set up, the launcher must be able to hold the balloon in up to 20 m/s gusts and 10 m/s sustained winds without falling over or damaging the balloon. The launchers must convey their state (arm/launch) to the operator wirelessly and using battery power. Moreover, the balloon launcher must have a system that can support 10-20 m long tethers to the gondola, as well as shorter tethers with in-flight un-winders. The launcher's design shall be easily manufactured and reproduced. The total cost of production of the launcher must be less than 1000 dollars. The following table shows each level of success for each category that are expected to be accomplished in this project.

Level of Success	Portability	Launch Capabilities	Balloon Security	Cost
Level III	• Assembly of this device can be performed by one person without the use of any tools • Device weight is no factor for a healthy adult • Deployment procedure is so obvious that the device can be assembled in 5-10 minutes • The device fits into a cylindrical case 25cm in diameter and 1m long.	• Launches 1 balloon with 1 payload or 2 balloons both connected to 1 payload • Control Comm: Wireless • Release Command Remote: On user • Reliability: 20 simulated test launches in 10 m/s sustained winds	• The BDS structure shall be stable and balloon launch without damage or entanglements in abnormal conditions for a typical colorado day in and around the mountains at about 20 m/s.	• The BDS shall be built within a proper facility using only bought components from the local hardware/electronics store for less than $1000 for a unit design.
Level II	• Can be assembled by a single person using nothing more than an allen key included and tethered to the device. • Device weighs less than 50 lbs and is reasonable to carry for most adults • Deployment procedure is simple and can be learned from an instructional card • The device fits into a single carrying case that can fit into the back of a sedan (55in X 36in) [11]	• Launches 1 balloon • Control Comm: Wireless • Release Command Remote: Off user • Reliability: 20 simulated test launches in 8 m/s sustained winds	• The BDS structure shall be stable and balloon launch without damage or entanglements in a typical colorado day in and around the mountains at about 8 m/s.	• The BDS shall be built within a proper facility using mostly bought components from the local hardware/electronics store. • Approximately half of the components will need to be outsourced and pre- ordered • All of which is under $1000 for a unit design.
Level I	• Can be assembled and deployed by a single user with the use of common tools like screwdrivers, standard wrenches, and pliers. • Device weighs no more than 50 lbs • Time to deploy is highly depended on user competency • The user can fit device into the average sedan, but does not fit into the desired carrying size	• Launches 1 balloon • Control Comm: Wired • Release Command Remote: Off user • Reliability: 10 simulated test launches in 1m/s winds	• The BDS structure shall be stable and balloon launch without damage or entanglements in a calm Colorado day in and around the mountains at about 1 m/s.	• The BDS shall be built within a proper facility using bought components from the local hardware/electronics store. • Approximately half of the components will need to be outsourced and pre- ordered • All of which is under $1500 for a unit design.

Table 1. Level of Success of BDS

Figure 4 Levels of Success

Level I requirements are those that generally would lead to a successful balloon launch without meeting all the customer requests. These include assembly and deployment by a single user with basic tools, weight around 50 lbs and a kit that would fit in a car. Launches could only handle 1 balloon with wired command communication hardware via an off user remote control and could launch 10 times reliably in 1-2 m/s winds. The structure would be stable and cause no harm to the balloon with wind speeds less than this limit, which is approximately the 25th (hourly) percentile wind speed during the non-winter months of the year [1]. Custom parts may make up half of the total parts number and manufactured cost could be as high at 1500 dollars.

Level II requirements build off Level I and get closer to meeting all the customers requests. Tools are reduced to just an allen key, assembly can be quickly learned from an instructional card. Wireless command communications are used instead of wired and reliability is verified in higher winds at 8m/s over 20 trials. Structure stability and balloon safety shall occur in higher winds at 8m/s, the average 90th percentile of hourly wind speed on the windiest day of each year, in Boulder, CO [1]. Finally manufacturing costs shall be within the 1000 dollar customer limit for a prototype.

Level III requirements meet close to all the customer's needs and requests. At this level no tools are required for assembly and weight is a non issue for the average adult being far less than 50 lbs. No instructions are required to build and assembly time takes 5-10 minutes. The full kit fits into a .25x1m carrying case. This system shall have the ability to launch a 2 balloon rigged payload using remote control on the user. Reliability shall be tested in 20 tests in 10 m/s winds. Structure stability and balloon safety must be verified in 20 m/s wind gusts. All parts for this level will be off the shelf.

B. Concept of Operations (CONOPS)

Figure 5 shows BDS's Concept of Operations (CONOPS) diagram. After receiving the BDS in it's travel case the user goes to the launch site via car or foot. Once at the site the user assembles the BDS taking approximately 5-10 minutes to complete. Once the BDS has been assembled, the user will load the balloon and attach the payload while the BDS is in loading configuration. Next, the user will proceed to put the BDS in launch configuration; the 'arm' and 'launch' commands will then be given while the user stands downwind of the BDS with payload in hand. Once the balloon is overhead, the user will release the payload. Once the balloon is away the user will disassemble the kit, return the contents to the travel case and vacate the site.

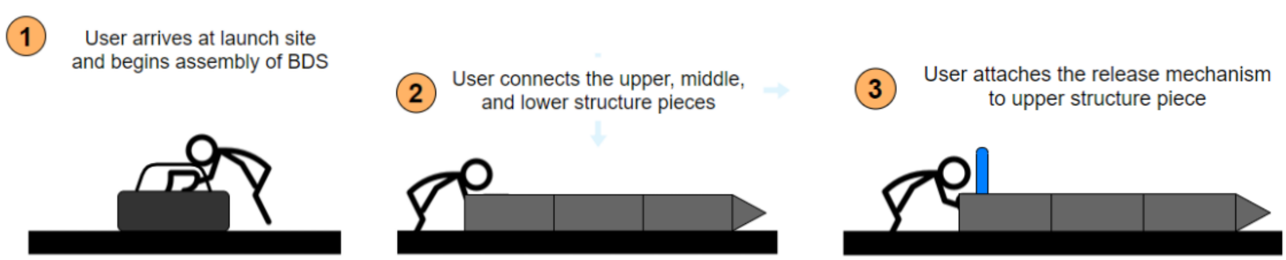

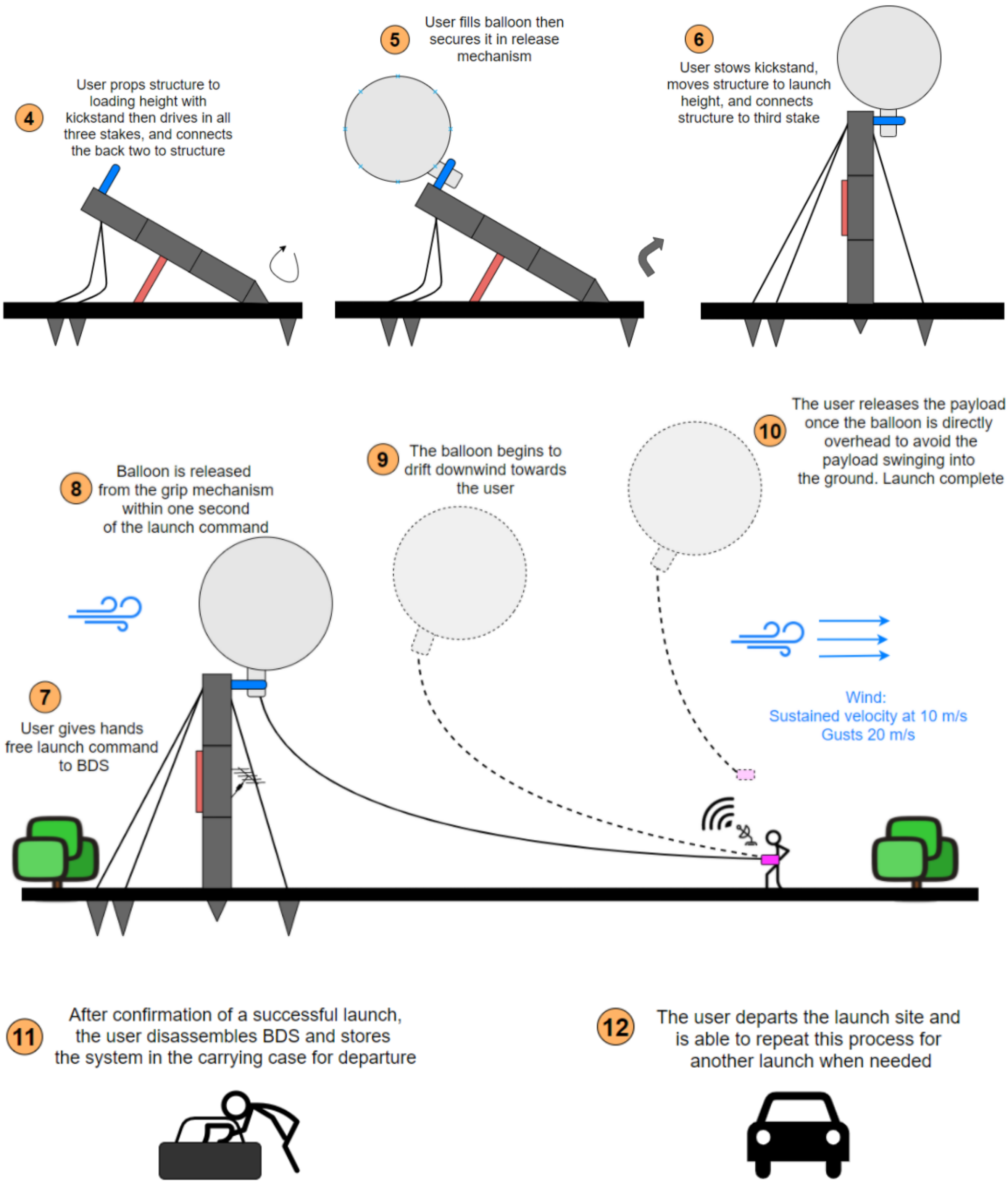

Figure 5 CONOPS for BDS

C. Project Deliverables

The tangible deliverables for this project can be broken into three categories. The structural deliverables contain everything important to the stability of the structure. They include the stakes, tie-downs, the kickstand, and mast. The structure can be disassembled into three one-meter-long pieces for ease of transport. The electrical deliverables contain the command and control for BDS. The electronics on BDS are controlled with an Arduino Uno. The user can send commands to BDS with an RF transmitter that is worn around their waist on a belt. The electronics box also include a switch and a speaker which act as safety and communication features for the user. The final tangible deliverable is the release mechanism. It sits at the top of the structure and holds the balloon in place until ready to launch. These deliverables are all packed into BDS's carrying case.

This project's deliverables were influenced by intangible elements too. The BDS must be easy to transport and set up by one person. These limitations impacted a number of design decisions, primarily weight, size and collapsiblity considerations. With everything in its carrying case, BDS weighs 33.2 lb-f; for reference the OSHA max safe lifting weight is 50 lb-f. The single user set-up capabilities influenced the CONOPS heavily and is the reason for many of the design decisions such as the kickstand and transmitter belt.

D. Functional Block Diagram

Fig. 6 illustrates the team's functional block diagram. After the setup process, the structure will be at its 3 meter height, with the balloon clamped within the electromagnetic gripper. The user will be on the ground, with the command transmission mechanism/button around their waist, and the payload will be tethered to the balloon. The user will initiate the deployment process by interacting with the button (*the arming stage*), and then pick up the payload with both hands. When the user is ready to deploy, they will press the button with their elbow. This sends a command to the transmitter, which communicates through radio frequency with the electronic system at the top of the structure. The receiver module and board will relay this command to the micro-controller (an Arduino Uno). Next, the micro-controller will actuate the relay to power the speaker feedback system, and to release the electromagnetic gripper. Thus, the balloon will be released, and the user will release the payload once the balloon drifts overhead. At the 3 meter height, the speaker and gripper are powered by a 12V battery pack. There is also an override switch, which opens the electromagnetic gripper without needing to rely on any RF communications. Further specifics of the hardware and their associated wiring connections are discussed in upcoming sections.

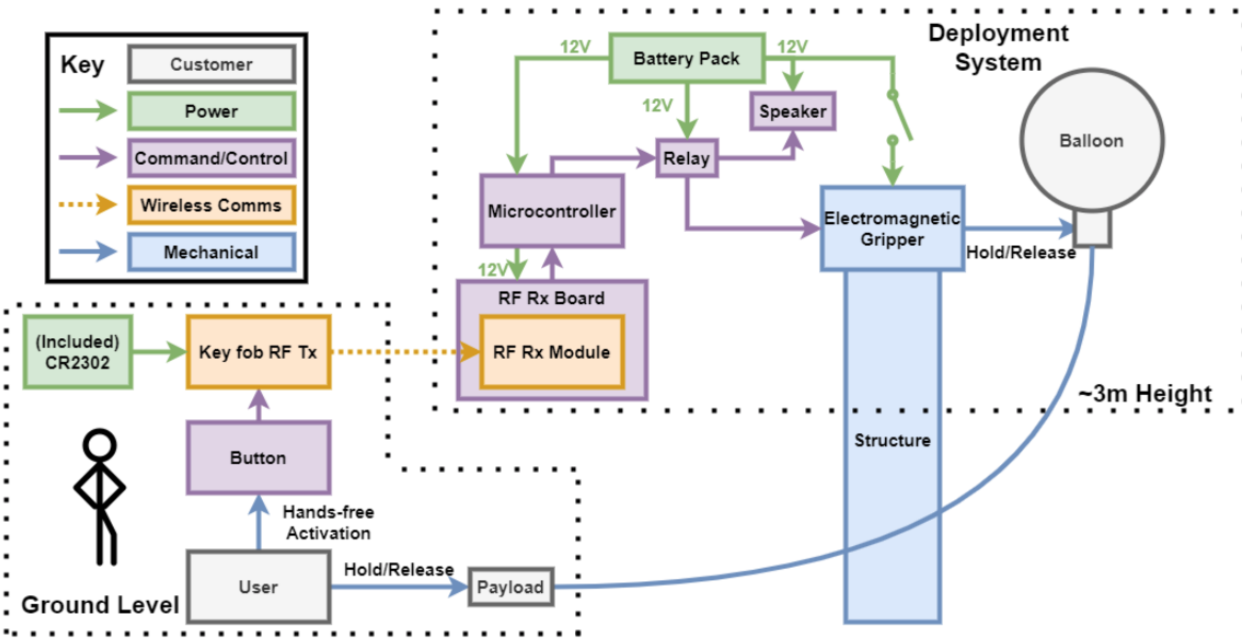

Figure 6 Functional Block Diagram

In terms of which elements are designed by the team vs which are acquired, all subsystems are designed by the team using off the shelf components with minimal customization required. The structure, release mechanism and command and control units are all designed to function and meet the customer requirements based on design and modeling by the team. With that said the tower bars, tower connections, support cables, stakes, hinges, foam, electronics and batteries will all be readily available from online sources. The only customization will involve 3D printing the release mechanism belt-mounted unit on the user, machining some parts of the release mechanism arms, cutting mast bars and kickstand legs and sharpening the bottom stake of the structure tower.

E. Functional Requirements

	Functional Requirements	Rationale/Explanation
FR 1.0	One person shall be able to set up with no tools required for assembly/disassembly.	Ease of use and self contained kit for the user to bring to site.
FR 2.0	The setup shall take less than 5 minutes to set up/disassemble.	Quick deployment of the balloon.
FR 3.0	The launcher (for each balloon) shall collapse into a cylindrical storage/carrying bag of 1 m length and 25 cm diameter.	Ease of transport.
FR 4.0	Balloons shall be held 3m or more above the ground and 6m apart in the case of a 2 balloon launch.	Avoid balloon ground damage or balloons becoming entangled.
FR 5.0	Payload shall not hit the ground during setup and deployment.	Avoid damage to payload instruments.
FR 6.0	The balloon deployment system shall hold 1 or 2 balloons and be launched within 1 s of each other.	Allow multiple deployments if required for data gathering.
FR 7.0	No heating of the launcher or sharp edges on the launcher. Launcher shall hold the rubber balloon neck (not tether).	Avoid potential damage to balloon
FR 8.0	The launching system shall function in 10 m/s sustained wind, with up to 20 m/s gusts.	Allow launches in a wide range of wind conditions.
FR 9.0	The system shall be hands-free (hands will hold payload) communication of commands/launcher status between user and launch device.	Allow single person launch with hands-free for payload release as balloon rises.
FR 10.0	Battery powered launcher/release mechanism.	Remote area launch capability.

Figure 7 Functional Requirements

There are multiple functional requirements that are necessary to achieve certain levels of success. One of the functional requirements being that the balloon shall be held 3 m or more above the ground and 6 m apart in the case of a 2 balloon launch. This requirement is for the avoidance of any contact with the balloon and the ground or any other objects as well as entanglement. Further related to avoiding damage from high wind launches, the next functional requirement is that the launching system shall function in 10 m/s sustained wind, with up to 20 m/s gusts. Since the payload is fragile and its operation key for HYFLITS data collection, it is necessary that the payload is held with both hands. Therefore, another functional requirement is the system shall be hands-free (hands will hold payload) for communication of commands/launcher status between the user and launch device. A similar functional requirement is that the launcher must be battery powered allowing remote launch capability. Furthermore, one person shall be able to set up the entire system with no tools required. In addition this set up shall take less than 5 minutes to complete. It should be noted that after subsequent conversations with the customer this requirement is flexible and not a hard limit. The launcher must also be able to collapse into a cylindrical storage/carrying bag of 1 meter in length and 25 cm in diameter to allow for transport in a compact car.

III. Final Design

Authors : Patrick Paluszek, Sebastian Urrunaga, Aufa Amirullah

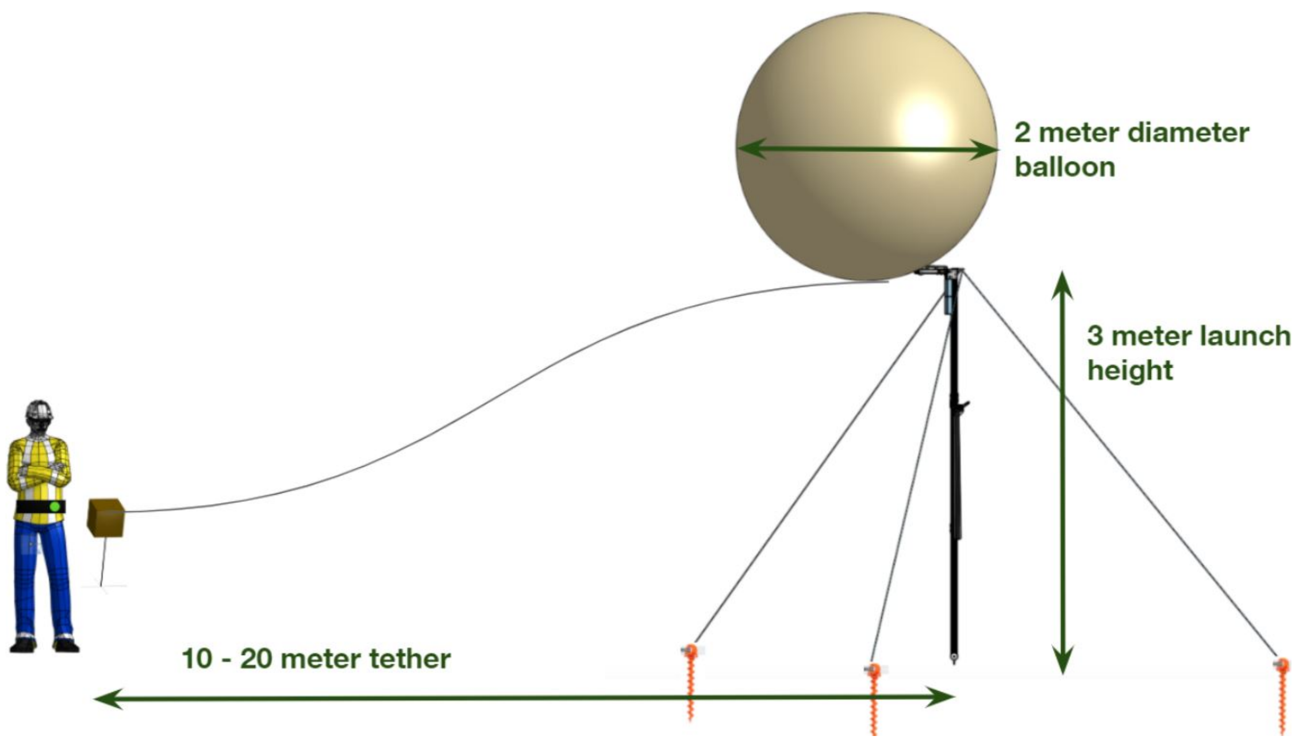

Figure 8 Full System

The overall design of the Balloon Deployment system is a 8020 aluminum mast with 3 adjustable nylon tie downs staked into the ground for stability as seen in Figure 9. This design helps fulfill a number of design requirements including ease of assembly and transport. The mast is made of three separate sections which are connected via brackets to form a three meter tall tower to meet our customer's requirements. They are tightened together with knob bolts allowing assembly to remain tool-free. At the bottom end of the structure is a stake to prevent the base from sliding in high wind conditions. The mid-section of the mast includes a kickstand to elevate the top end of the structure while the balloon is being loaded to keep it off the ground. The top section of the mast includes three D rings where the the three tie downs are connected to the structure to provide stability, shown in Figure 11. These tie down ropes connect from the D rings to the screw-in-stakes at the ground. The screw-in-stakes are located 2.64 m from the tower and at 120 degrees from each other on the ground around the base of the mast. Meanwhile, the forth side of the mast (w/out a d-ring) is where a dynamic pivot is attached to help maneuver the release mechanism as it weather vanes downwind while grasping the balloon. These components at the top of structure are domed off with foam padding to satisfy the teams balloon safety requirement.

Figure 9 Structure CAD

Figure 10 Structure

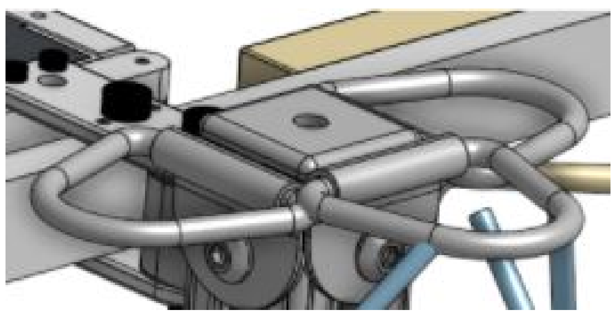

Figure 11 Top of Structure

The release mechanism design satisfied a number of requirements including balloon loading by a single user, ensuring the balloon would not be damaged, and that the system shall function in ten meter per second sustained winds and survive twenty meter per second gusts. Single user balloon loading was achieved with the use of a remove-before-flight pin to arrest the degree of freedom. This allowed one of the swinging arms of the release mechanism to be held in place by the balloon neck as it is guided by one hand. The other hand shall then bring the other swinging arm to come in contact with the permanent electromagnet. This swinging arm contains a smooth piece of ferromagnetic steel to be engaged with the permanent electromagnet. These two swinging arms have each a fiction fit, 3D printed structures that houses a rubber padding. The right swinging arm also houses the piece of ferromagnetic steel while the left swing arm comes in contact with permanent electromagnet. These rubber padding are flush with the permanent electromagnet and piece of ferromagnetic steel to ensure the balloon neck does not get pinched in between the sections.

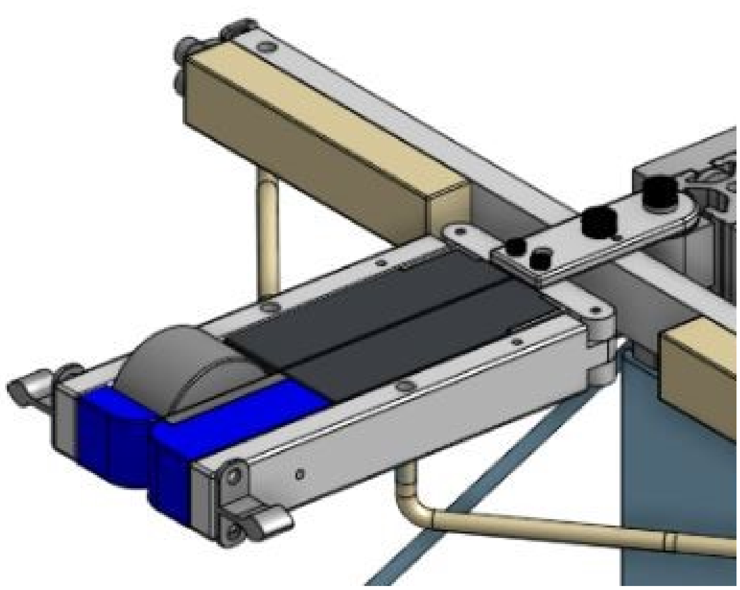

Figure 12 Release Mechanism Showing Dynamic Pivot

The structure of the release mechanism resembles a slingshot. It is attached to the dynamic pivot that allows for a total of 108 degrees of rotation to weather vane with the wind. One end holds the smaller back plate that pivots the left and right swinging arms. While the other end of the dynamic pivot is T-bolted into structure. Inside the dynamic pivot, near the middle portion is the long back plate. To include this section, the team had to customize the dynamic pivot such that it allowed a dowel pin to be inserted between both the upper and lower sections of the pivot; sandwiching the long back plate in between. This long back plate acts as a back board for the incoming swinging arms. It arrests the swinging motion of the arms and at the same time prevents the arms swinging back into the balloon neck and venting valve. It does this through the connection of surgical tubing. It first acts like a extended spring to rotate the arms out of the way of the balloon neck. It then forces the arm to come to rest against it's foam padding on the long back plate. Lastly, if there is any whiplash, the surgical tubing then acts as a restraint, preventing the swing arm from rotating back away from the back plate. All metal edges and protrusions were designed such they were out of the way of balloon or chauffeured and smoothed if any chance of contact was present. The long back plate was then wrapped in foam tubing to further ensure balloon safety. The forcing mechanism, including the surgical tubing and pins attached, are underneath the release mechanism.

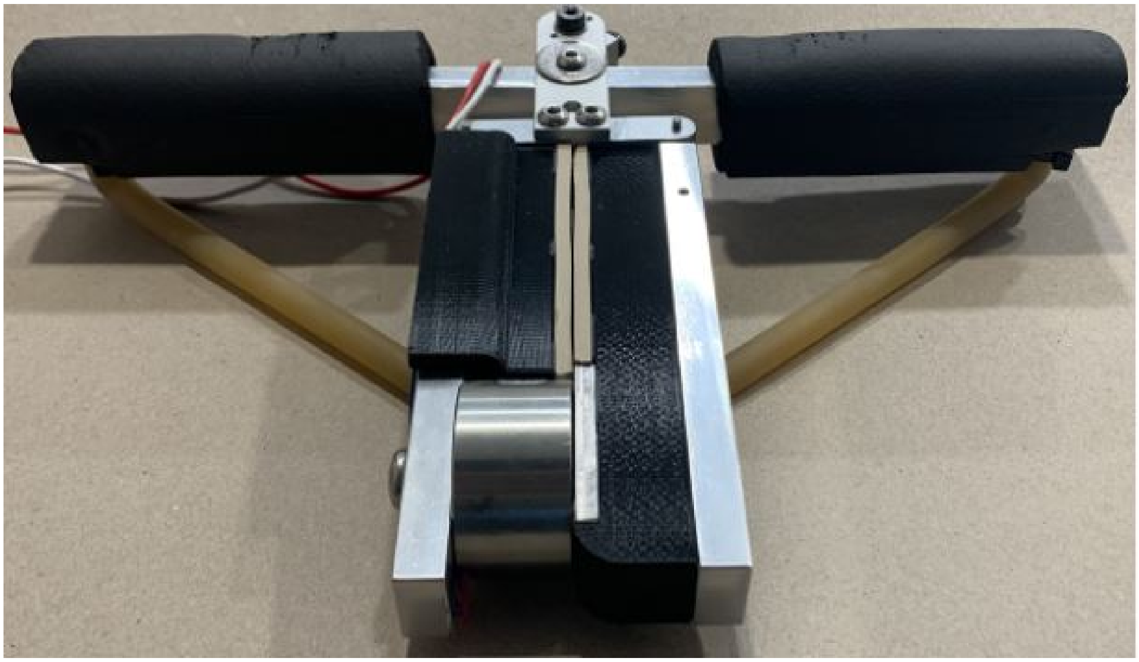

Figure 13 Release Mechanism

The forces expected on the balloon would then need to be restrained by the release mechanism and at the same time ensure balloon safety. The rubber padding used was to obtain a sufficient coefficient of friction and at the same time be flexible enough to keep the balloon neck safe with large forces. The balloon neck stretches, therefore the balloon neck is brought down to the base of the the sphere of the balloon. This process is not perfect and therefore an additional model of dynamical force was added to the maximum force the balloon can expect. In addition, a dynamic pivot was used to help align the release mechanism with the wind direction. This degree of freedom was needed to help reduce the chance of balloon damage if a crosswind pushed the balloon against the structure.

The Command and Control subsystem was designed and developed to deliver functional requirements including: multiple deployments, no damage to the balloon, hands-free operation, and remote area launch capability. These requirements were achieved by incorporating the use of RF signal and integrating the hardware with software development to allow the user to command and control the launcher during balloon deployment missions. The Command and Control subsystem was divided into two parts: a transmitter and a receiver. For the transmitter, it was equipped with a 315MHz key fob transmitter to send the RF signal. This key fob was rewired with an arcade button and housed inside a 3D printed belt-clip compatible box. The transmitter system can be used by attaching it to a belt or loop near the user's waist to accommodate a hands-free deployment via the user's elbow. The receiver system is housed in a separate electronic box which is attached to the support structure underneath the release mechanism. Inside the electronic box are an Arduino Uno, an RF module, a relay shield, and a current sensor. In addition, a speaker, an override switch, and a power switch are mounted to the side of this box to provide audio feedback to the user. All components are simply wired and powered by the 12 V rechargeable battery pack. The override switch was specifically designed to avoid potential damage from premature release by the user. The override switch allows the electromagnet gripper to easily be opened during setup or special circumstances. The switch bypasses all other components and directly powers the gripper from the battery. This means that if the override switch is flipped, the gripper is forced open. Otherwise, the system is controlled through aforementioned "arm" and "deploy" protocol. Fig 14 below is the complete final design of the Command and Control subsystem.

Figure 14 Command and Control Final Design

This final design is capable of sending an RF signal to command balloon deployment with a maximum range of 23 meters (75.4 feet). One of the main concerns of the overall project was the power consumption within the command and control subsystem, i.e., how often the battery needs to be recharged. The initial prediction was that using 12 V battery with 6.8 A current draw would only give about 23 launches. However, this is no longer an issue as the test result show that BDS could launch for hundreds of deployments, satisfying the functional requirement regarding multiple deployments.

The total balloon deployment system weights in at roughly 15 kilograms(33.2 lbms) and when disassembled and packed measures 1.1m x 0.25m x 0.25m in dimension. The system can be made to be exactly 1m in length per customer requirements, however this adds additional time for set up. The 10 cm additional length does not compromise the transport-ability of the system and therefore was traded for faster set up.

IV. Manufacturing

Authors: Austin Konnath, Aufa Amirullah,Chenshuo Yang

A. Manufactured Parts

A..1 Structures

The structure manufacturing consists of cutting 3 1.5"x1.5" 8020 aluminum bars to 1 m length as show in in Figure 15. The bar that will be the base also requires threads to be cut into the center longitudinal hole in the bar for a 3/8-16 inch thread to secure the base stake. This base stake is made from a 3/8-16 threaded aluminum rod that is then machined into a cone on one half of it's length, as seen in Figure 16. All surfaces require smoothing after cutting besides the base stake.

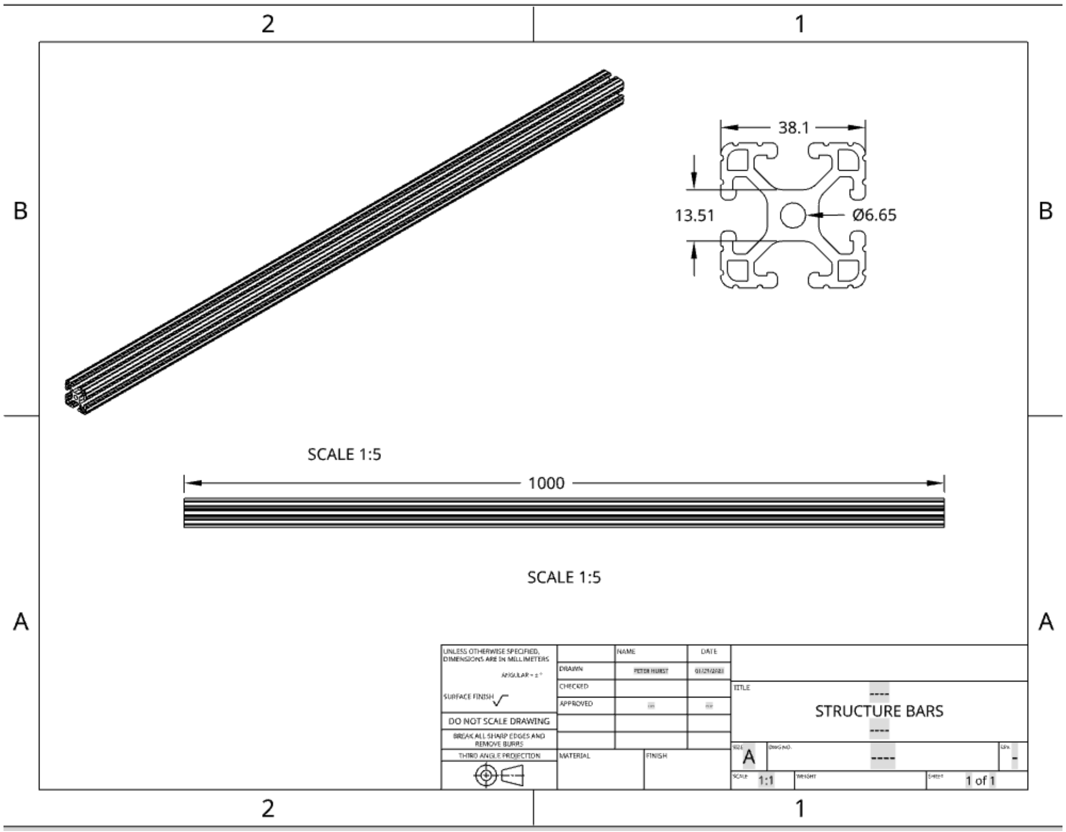

Figure 15 Mast Bars Drawing

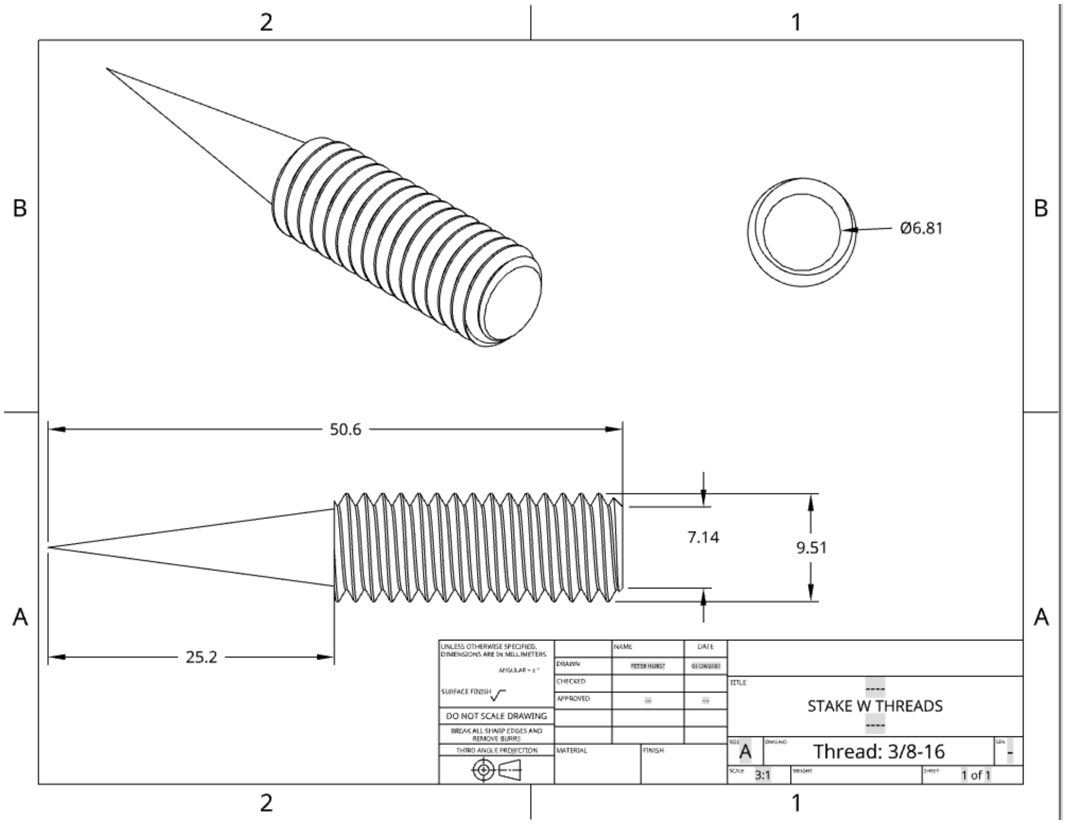

Figure 16 Base Stake Drawing

The kickstand component requires cutting the 2 1.5"x.75" 8020 bars shown in Figure 17 to 1 m lengths as well. After cutting the ends of the kickstand should be smoothed.

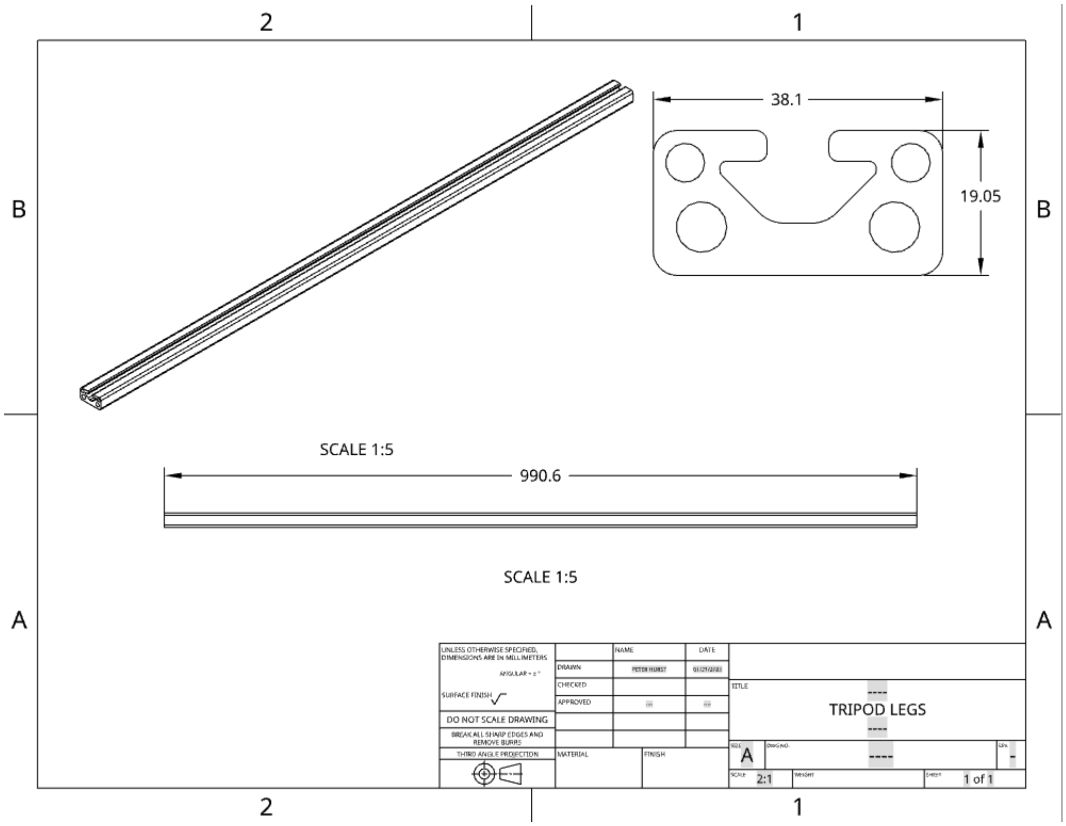

Figure 17 Kick Stand Drawing

Assembly begins with installing the connecting plates that will allow the mast to be assembled as seen in Figure 18. These consist of the T-slotted framing silver surface brackets (6" long) purchased using 2 of the end-feed double nut/flanged button head (5/16"-18 thread) for each connecting plate.

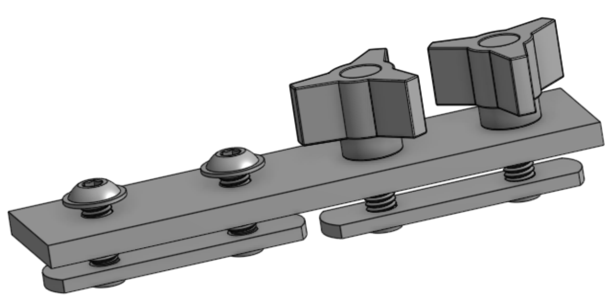

Figure 18 Mast Connections Plate Assembly

Each mast junction consists of 2 plates oriented perpendicular to each other, as seen in Figure 19. Each plate should be placed with 3" of overlap on the mast with 3" overhanging to allow for the other bar to be slotted in. One one side 5/16"-18 Allen bolts are used for the permanent connection to the 8020 mast bars while on the opposite side three arm knob bolts with 5/15"-18 thread and 3/4 long (w/1 1/2" head diameter) are used for the side that will be removable. The Allen bolted side of the plate is tightened down to form a permanent connection.

Figure 19 Mast Connections

At this point the base stake can can be threaded into the bottom section of mast. For transport the base stake should be threaded with the sharp end pointing into the 8020 mast section and can be un-threaded, flipped, and then re-threaded with the sharp end pointing out for raising the structure, as seen in Figure 20

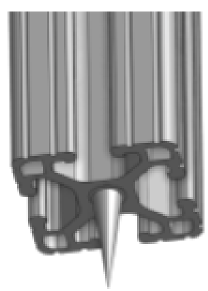

Figure 20 Base Stake Thread In

The next step is assembly of the kickstand. The kickstand consists of 2 1m 8020 bars cut previously and then connected to t-slotted framing pivots w/locking inline/perpendicular pivots. These allow the kickstand to be folded alongside the mast and then deployed for balloon loading. The arms allow the pivots to be tightened to lock in place. These pivots are shown in Figure 21

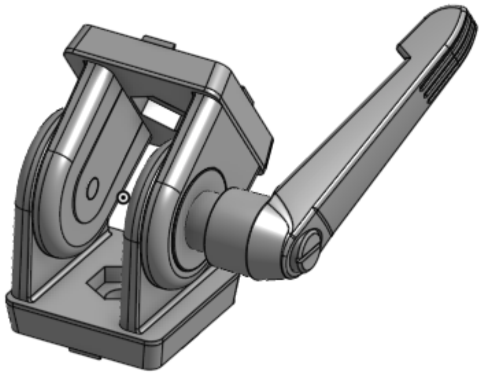

Figure 21 Kickstand Pivot

The kickstand pivots are bolted to the top of the mid section mast opposite the connection plates as seen in Figure 22. The other end is then bolted to the kickstand bars via a corner bracket. These connections are made via 2 of the end-feed single nut/flanged button head (5/16"-18 thread) bolts with one connecting the pivot to the mast via the slot in the mast and another connecting the bracket to the kickstand via the slots in the kickstand. The other end of the bracket uses the same bolt but with a standard/non-slot fit nut to connect the bracket/kickstand bar to the other end of the pivot.

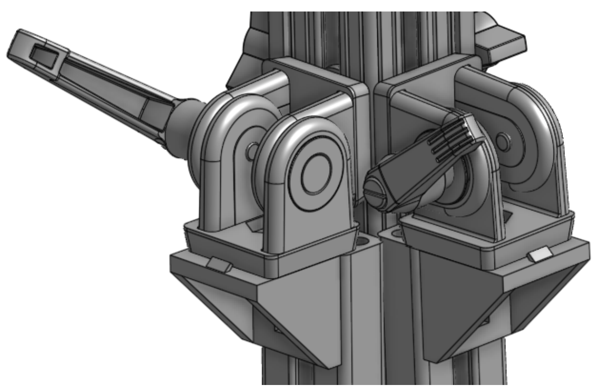

Figure 22 Kickstand Pivot Assembly

The next step is attaching the 3 d-rings with 3 of the end-feed single nut/flanged button head (5/16"-18 thread) bolts to the top of the top mast as seen in Figure 23. Here the end feed nuts are placed in the channels with allen bolts used to tighten the d-ring brackets against the 8020 top section of mast. The 4th side remaining is used to attach the release mechanism.

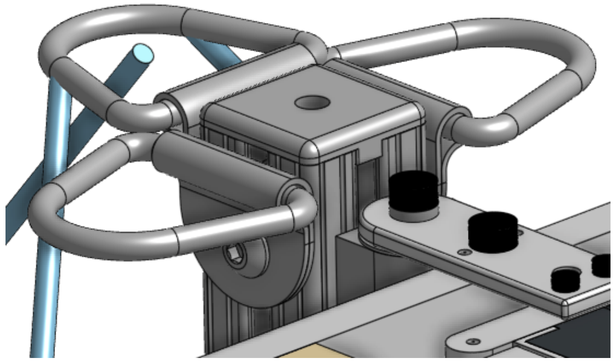

Figure 23 D-ring Attachment

With the d-rings attached the protective foam cap can be attached. The cap is 8 in x 8 in x 2 in and sits on top of the structure to prevent the balloon from contacting the d-rings, carabiners or tie-down rings, as seen in Figure 24. 4 holes should be punched in the foam above the 2 side facing d-rings to thread zip ties through the foam and then around the d-rings to keep the foam in place. The holes should be centered along a side of the foam, spaced at .25 inches inboard from the side arranged in a square, with each hole at 1.5 inches apart. Once attached the foam should overhang the d-rings but be flush with the side of the structure where the release mechanism is to be attached. See Figure 25.

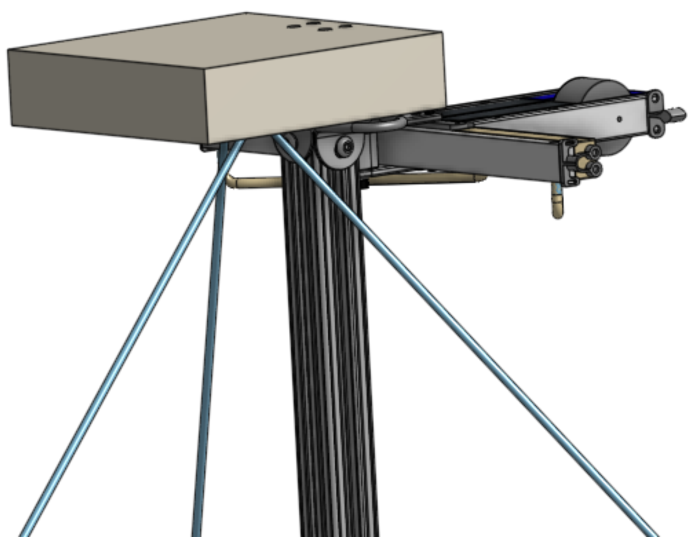

Figure 24 Foam Protective Balloon Cap

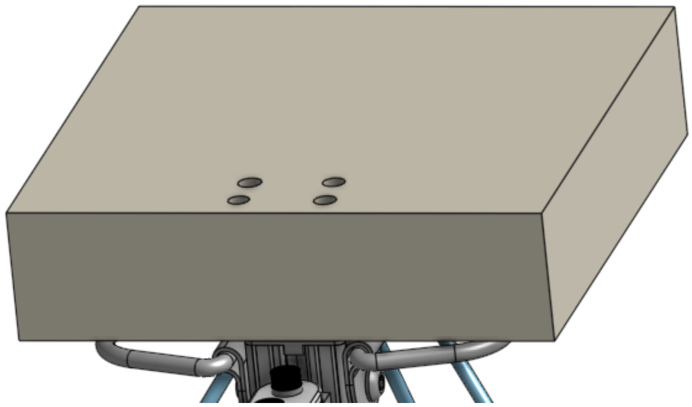

Figure 25 Foam Cap Hole Placement

The next step is the creation of the staking template. This consists of nylon rope and 4 stainless steel rings which allow the user to quickly place the screw in stakes in the correct position for successfully raising the structure. 3 sections of rope 8.66 ft in length are tied from the center ring to each of the 3 corner rings with 3 15 ft pieces of rope tied between each of the corner rings as seen in Figure 26

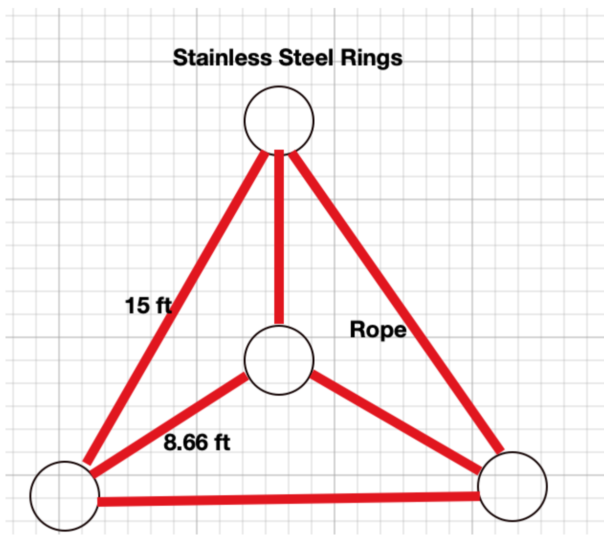

Figure 26 Stake Template

A..2 Release Mechanism

The release mechanism relies fairly heavily on manufacturing. The swinging arms which close around the balloon are cut from stock aluminum on a CNC mill. Custom hinges were designed into the model of the arms which are fitted with their attachment point on the small back plate and connected using slip fit steel alloy dowel pins to allow them to swing freely. The tolerances for these two fitted pieces allow for minimal friction. Several holes need to be drilled into the swinging arms to attach additional parts such as the electromagnet and 3D printed inserts. In the left swinging arm, a size M8 hole is drilled and tapped to attach the electromagnet. In the right swinging arm, a size 1/4-20 hole is drilled and tapped to secure the steel plate the electromagnet latched to. In both arms, size M4 holes are drilled and tapped to secure L-brackets for preventing over rotating the arms in the wrong direction. These holes were part of our original design, however they were found to be unnecessary for the mechanism to function. Holes are drilled in the bottom of each arm to be slip-fit for 1/4 inch steel allow dowel pins in order to mount the latex tubing. Lastly, 1/8 inch holes are drilled for steel alloy dowel pins to be slip-fit in each arm for the loading configuration as well as to create each arm's hinge.

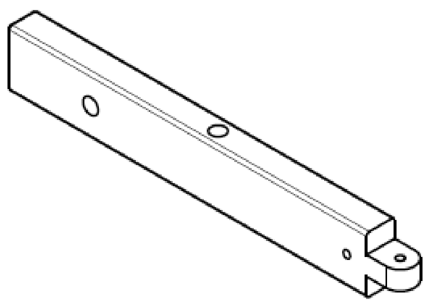

Figure 27 Left Swinging Arm

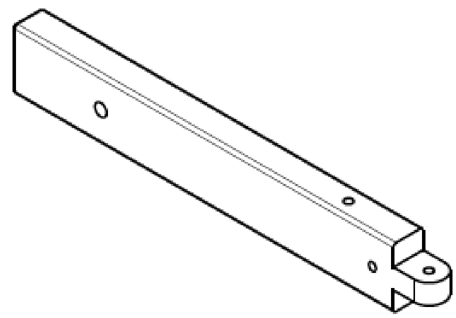

Figure 28 Right Swinging Arm

The small back plate connected to both swinging arms is also cut from stock aluminum on a CNC mill. This piece is also cut to function as the other half of each custom hinge for the swinging arms with 1/8 inch holes drilled for the dowel pins. Additionally, two 1/4 inch holes are drilled towards the center in order to attach the piece to the dynamic pivot using 1/4 inch bolts.

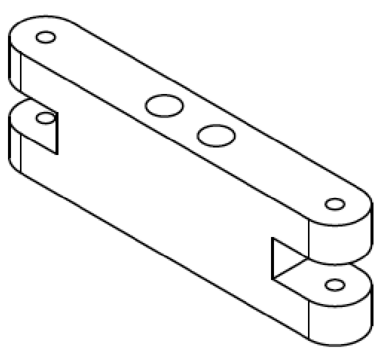

Figure 29 Small Back Plate

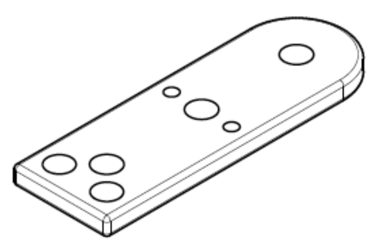

Figure 30 Dynamic Pivot Arms

The dynamic pivot comes prefabricated from 80/20, but modifications are made to attach its arms to the long back plate and small back plate. Two 1/4 inch holes are drilled for attachment to the small back plate and two 1/8 inch holes are drilled for slip fit pins to prevent angular motion between the long back plate and the pivot arms.

The long back plate is cut from stock aluminum on a CNC mill. One 0.257 inch hole is drilled in the center for a bolt to secure the back plate to the dynamic pivot arms and two 1/8 inch holes were drilled just outside the center for the dowel pins to prevent angular motion. Additionally, two 1/4 inch holes are drilled towards the outer ends to friction mount the back ends of the latex tubing to the long back plate.

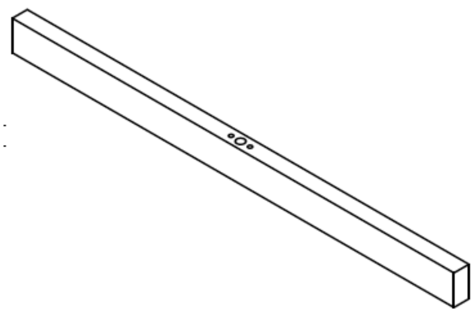

Figure 31 Long Back Plate

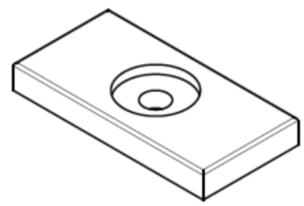

Figure 32 Steel Plate

The last manufactured part of the release mechanism is the steel plate to serve as a latch for the electromagnet. The general shape of the plate is cut from stock steel in a CNC mill. One 1/4 inch hole is drilled through the center of the plate for mounting to the right swinging arm. This hole is also beveled out to allow the bolt head to fit flush with the inner surface of the plate.

All metal edges of the release mechanism parts are lightly rounded to prevent creating sharp edges which could damage the balloon. All manufacturing of the previously discussed parts was done in the SMEAD Aerospace Machine Shop by shop staff. The last remaining manufactured parts were made on our project manager's 3D printer. These pieces were designed to be friction fit to the swinging arms. The insert on the right swinging arm is designed with a 1/4 inch hole for the steel plate's securing bolt to pass through. Once all parts were manufactured, the entire release mechanism was assembled using the purchased parts in the following sections.

A..3 Command and Control

The manufacturing for Command and Control subsystem is divided into two parts: hardware and software. All Command and Control components were provided off-the-shelf, hence the team bought all the necessary components online. For hardware parts, the Command and Control subsystem easily breaks down into two portions: a transmitter and a receiver. The transmitter is a rewired RF key fob to an arcade button which is covered within a 3D printed housing. This transmitter system can attach to a belt on user's waist to enable a hands-free operation. While the transmitter sends the RF signal, the receiver system receives the RF signal to control the electromagnetic gripper and hence the deployment. The receiver system is housed in a separate electronic box with a dimension of 7.25 x 5 x 2.2. inches. The electronic box is attached to the support structure and under the release mechanism, as shown in Fig 33 and contains an Arduino Uno, an RF module, a relay shield, a current sensor, and a 12V battery pack. In addition to the receiver system, a speaker is provided to provide audio feedback to the user and is mounted to the side of the electronic box alongside the power switch and the override switch. All these components are simply wired and powered by the rechargeable 12V battery pack as shown in Fig 34 and more detailed electronic schematic is shown in Fig 35. In this receiver system, the RF module is used to receive the RF signal and provide the wireless remote control system, while Arduino Uno is used to process all the wireless command lines that comes from the RF module and passes it through the relay shield. The relay shield is equipped into the system to output higher voltage from the Arduino which then is used to deactivate the permanent magnet gripper. The override switch is used for opening the gripper while attaching the balloon on the ground and to ensure that the balloon does not prematurely launch. A power switch is added to the system to provide more flexibility to the user to control the power of the system.

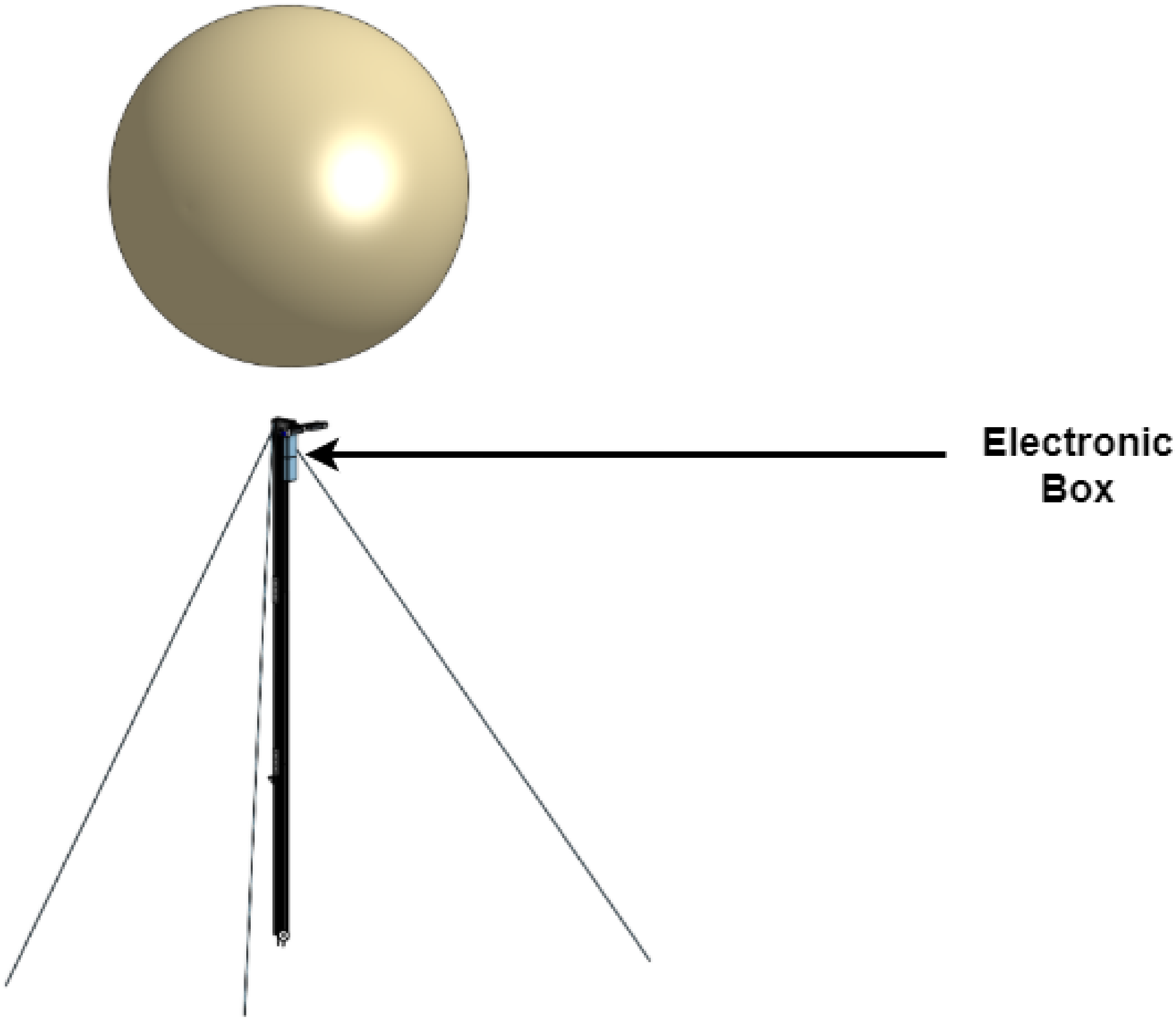

Figure 33 Command and Control subsystem location

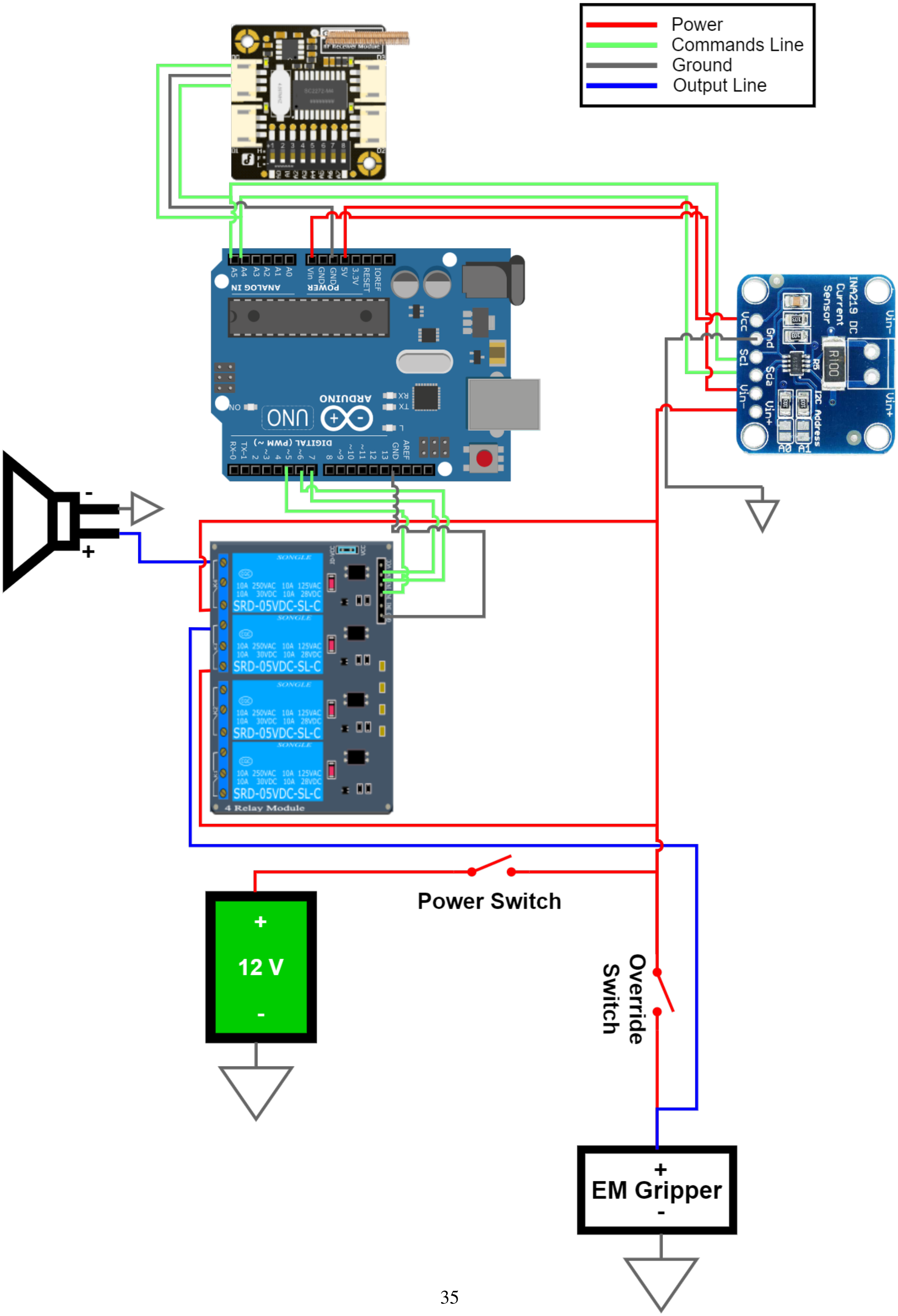

Figure 34 Wiring Diagram

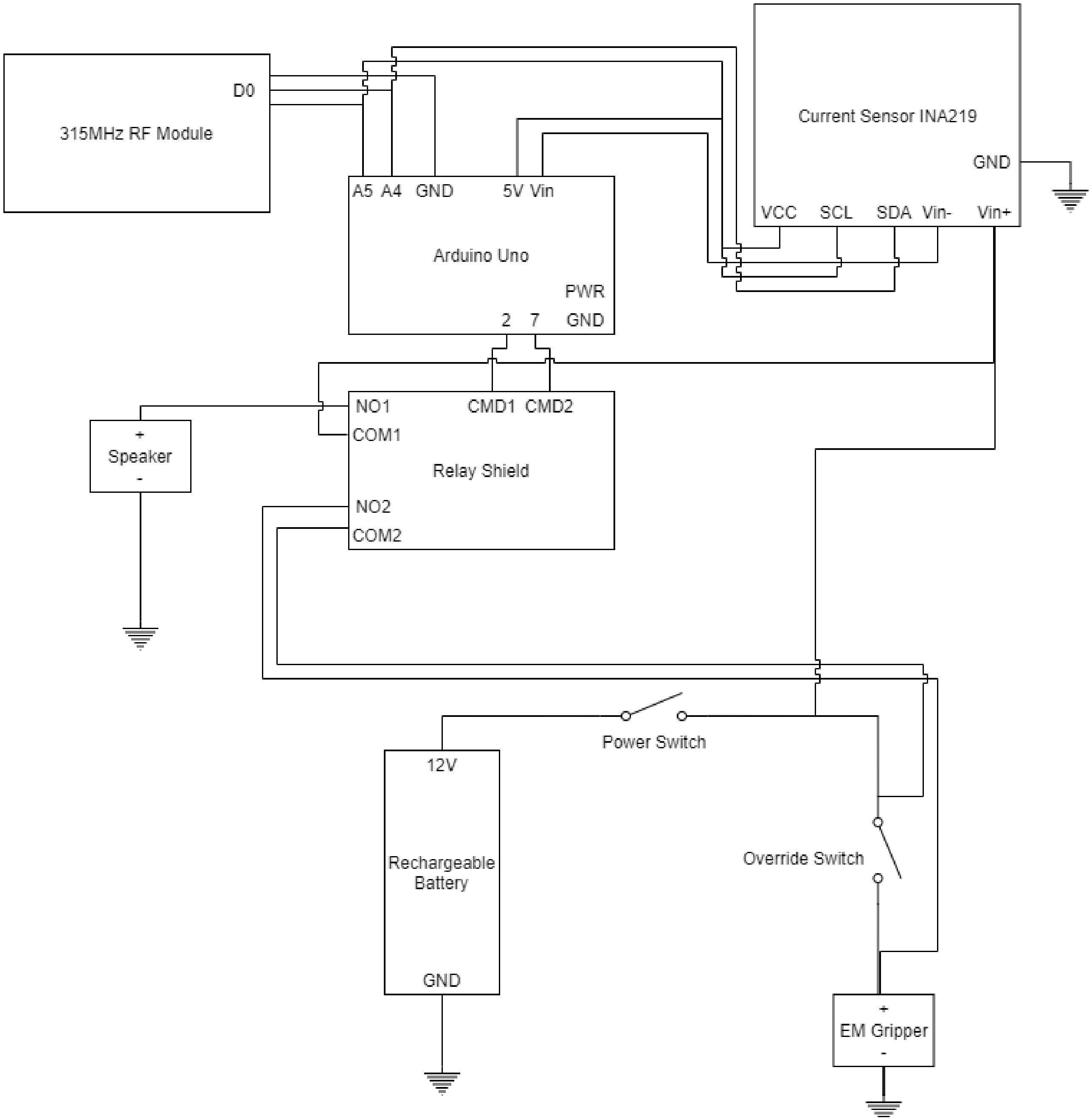

Figure 35 Electronic Schematic

Secondly, BDS considers a moderate reliance on software and the use of software is to support as well as integrate the hardware parts to operate autonomously and send user commands wirelessly. The software of BDS is programmed and developed on Arduino's software platform called Arduino IDE. Arduino IDE adopts a C++ programming language with more abstraction built in functions in the hardware interfaces which makes it very straightforward to use. The overall Arduino Code for RF release system is provided in the Appendix section. BDS is programmed with 4 functions within the software which runs different task, for instance:

1) deactivateFob is a function to turn on and off power of the system
2) deactivateGripper is a function to deactivate the permanent magnet gripper, this allows the system to open the gripper automatically
3) beep is a function that is specifically designed for the speaker system to notify the user of the following three cases, with unique and identifiable tones:
    1) The system has been armed, after the user first holds down the transmitter button.
    2) The system is about to deploy, after the user presses the transmitter button from the "armed" stage.
    3) The battery in the receiver system is low.
4) batteryLevel is a function to read the level of the voltage of the battery which is also read by the current sensor INA219.

Fig 36 below is the flow chart that outlines the process of the code will be handling in the Command and Control subsystem. The command and control subsystem requires two stages in order to successfully operate: arming and deployment.

Before the user begins the balloon loading, the user will turn on both the power and the override switch. Once the loading process is done, the user presses the button on the remote. The arming stage starts when the user presses the button, i.e. the transmitter sends the RF signal to the receiver. Using the RF module, BDS captures the RF signal from the transmitter. This signal is then transferred to the Arduino Uno where this device processes all the command lines for wireless link command. The relay shield board which is stacked below the Arduino shall output higher voltage from the Arduino using digital IOs with external 12 V supply which comes from the battery pack. When the RF signal has been processed by these electrical components, the Arduino commands this processed RF signal to output a sound through the speaker while it is powering the electromagnet gripper.

The deployment stage starts when the user hears the audio feedback from BDS, at this time the user shall press the button for the second time to send another RF signal to the receiver. The second signal shall command the Arduino to stop powering the electromagnet gripper. It is important to note that if something wrong happens at this stage, the user shall turn off the power in order to disarm the whole BDS system and reset the arming procedure from the beginning. The final step of deployment stage is when the release magnetic gripper is deactivated, i.e. the gripper is opened and at the same time the user shall hear final audio feedback indicating that the gripper is successfully opened.

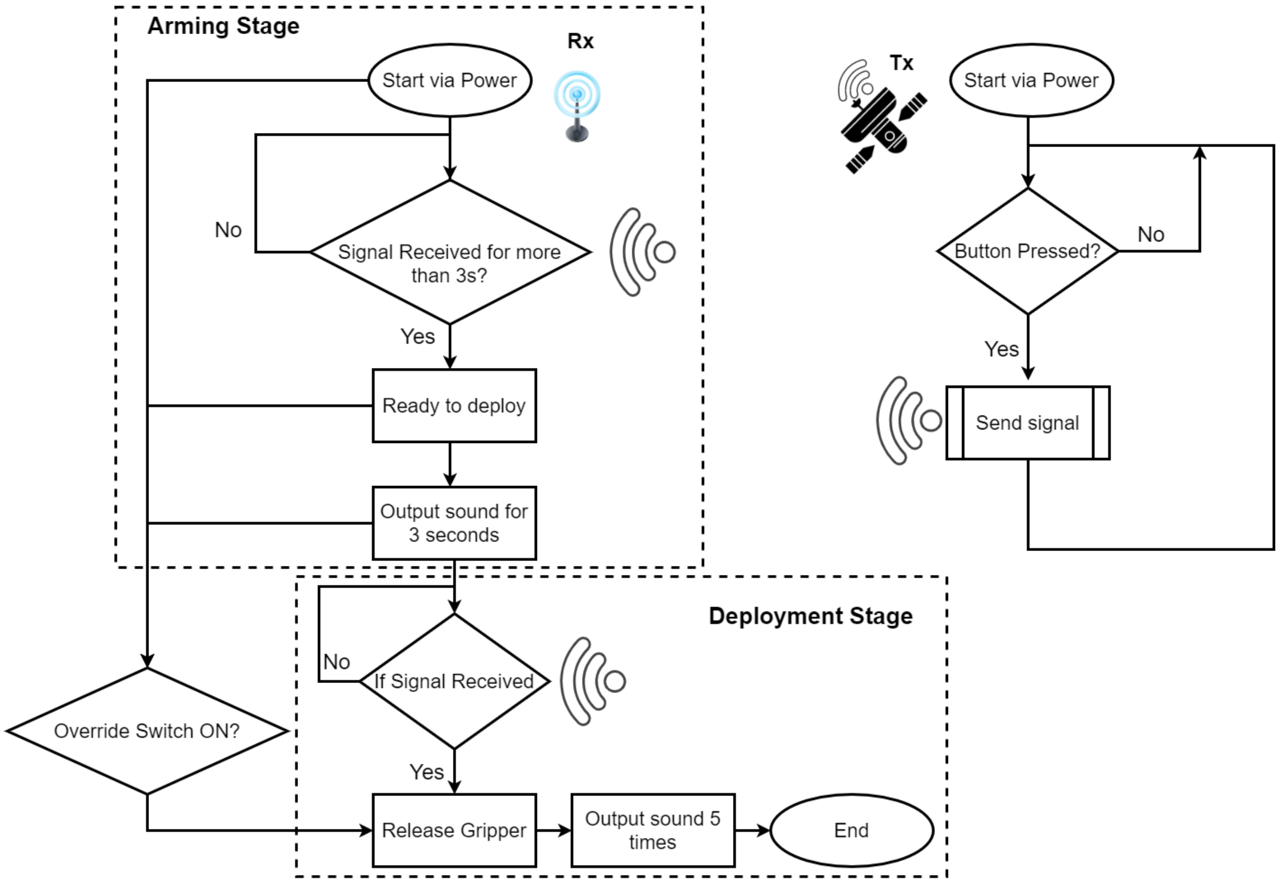

Figure 36 Hands-free Operation Flow Chart

B. Purchased Parts

Authors: Chenshuo Yang

The following subsection is the list of materials that have been purchased for each subsystem.

B..1 Structures

- 3 meters 8020 Aluminum Bar: T-Slotted Framing Double Six Slot Rail, Silver, 3" High x 1-1/2" Wide, Holl
- 3 Support Tie down : Tie Down with Rings, Quick-Tight, 1" Wide, 6 Feet Maximum Length, Nylon
- 3 Ground Anchors :Weight 1.8oz, Length 9 ½", Diameter ⅞", Material Recycled Polycarbonate
- 3 Tie down rings : Tie-Down Ring Zinc Plated Steel, Steel Base
- Aluminum Base stake
- 8 Thumb Screws
- 4 Bar Connectors : T-Slotted Framing Silver Surface Bracket, 6" Long for 1.5" High Single Rail

Figure 37 Structures purchased parts

B..2 Release Mechanism

- Electromagnet (EML50mm-12)
- Trident Bulk Latex TUBING Sold by The Foot - 1/2" Outer Diameter, 1/8" Inner Diameter
- 10 series standard 90 degree dynamic pivot assembly with dual straight arms
- EML50mm-12
- PLA Filament
- ¼ x 1 dowel pin alloy steel
- ⅛ x 1 ¼ dowel pin alloy steel
- ⅛ x 1 dowel pin alloy steel
- ¾ in x ½ in steel corner brace with zinc finish
- Ring Pin, Cotterless, Steel, C1144, Zinc, 3/8 in Pin Dia., 1 5/8 in Usable Length, PK 5
- Grab, Non-locking, Grab Catch, 1 15/64 in, White Plastic
- Armacell ¾ in. x 6 ft. Rubber Self-Seal Pipe Wrap Insulation-HSTO
- 1/4 in.-20 tpi Grade 5 Zinc-Plated Flange Nut (2-Pack)
- 1/4 in.-20 tpi x 60 mm Narrow Black Connecting Bolt (4-Pack)
- 1/4 in. x 1 in. Metallic Stainless Steel Fender Washer (3 per Pack)
- 1/4 in. Zinc-Plated Split Lock Washer
- 2 in. Thick Multi-Purpose Foam
- High Performance 13.5 oz. Spray Adhesive
- Gound Low-Carbon Steel Sheet, 3" x 3" x 1/4"
- Super-Cushioning Polyethylene Foam Sheets and Strips (24" x 18")
- Multipurpose 6061 Aluminum, 1/2" Thick, 2" x 48"
- MTR MACH SCW PN HD PHI SS8M-1.25x30M
- Loctite 242 Threadlocker Blue 0.2 OZ
- Machine Screw Flat HD 4M-0.7x12M Stainless Steel
- Hex Nut GR-8 ¼ Zinc
- ⅜ Hitch Pin
- SCK Cap SCW Button HD SS ¼-20X2

Figure 38 Released Mechanism purchased parts

B..3 Command and Control

- Arduino Uno (1 unit)
- Arduino Relay Shield (1 unit)
- 12V Rechargeable Battery Pack (1 unit)
- Speaker (1 unit)
- Toggle Switch (2 unit)
- Banana Plug and Receptacle (2 units)
- Remote Wireless Keyfob 315 MHz (1 unit)
- RF module (1 unit)
- Large Arcade Button with LED (1 unit)
- 3D Printing Material (for button housing)
- Plastic electronic enclosure (Electronic box) (1 unit)
- Wire 20/2
- INA219 Current Sensor (1 unit)

Figure 39 Command and Control purchased parts

C. Integration

Authors: Chenshuo Yang

C..1 Component Integration

Integration begins with adding the release mechanism and command and control electronics box onto the top bar of the structure. As shown in Fig 40, the release mechanism is bolted into the T-slot mast bar at the top of the structure. As mentioned in the final design section, the swinging arms of the release mechanism are released by an permanent electromagnetic, which is controlled by the electronics within the blue boxes below the release mechanism. Two wires connect the release mechanism with the electronic box to achieve the demagnetization when current flows. In order to have a better signal receiving range, the electronic box is bolted at the mid section of the structure tower (2m above the ground), and the antenna is fixed on the outside of the box to further improve range.

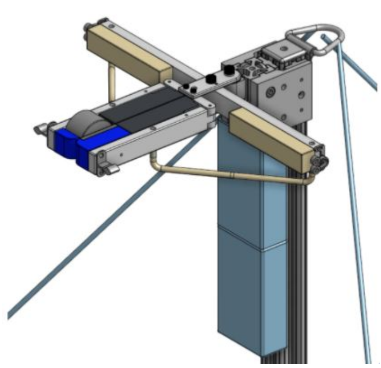

Figure 40 Release Mechanism and Command Control electronic box

C..2 Setup Procedure

1) Assemble tower: Slide top of base bar into bottom of kick-stand bar. Tighten knobs on bottom of kick-stand bar. Slide top of kick-stand bar into bottom of D-rings bar. Tighten knobs on bottom of D-rings bar.
2) Thread-in base stake: Locate bottom of base bar. Unthread stake, turn stake 180 degrees then re-thread into base bar.
3) Lay staking template on ground
4) Screw in stakes at 3 corners of template: Place stakes at corners of template. Hand thread stake into ground and then use plastic tube in stake eyelet for leverage
5) Deploy kickstand
6) Position top of mast at center of template
7) Clip tie down support to D-ring on top of mast
8) Clip opposite ends of tie-down to stakes
9) Ensure tie-down cams loosened to knot
10) Turn on electronics box: Flip power switch to "on", if release mechanism arms need to be separated, flip override switch.Then clip remote to user for elbow activation
11) Load balloon in release mechanism: Ensure release mechanism open, place balloon in release mechanism with foam valve tube facing away from mast and balloon neck clamped as close to base of balloon as possible. Push release mechanism arms together until magnet clicks closed
12) Raise mast, place base stake at center of template
13) Tighten tie-downs, ensuring mast straight
14) Walk back with payload, begin launch command

V. Verification and Validation

Authors: Grant Norman, Peter Hurst, Austin Konnath

In this section, we explain how the physical design was verified against our engineering models. The three models of interest are the wind loading model, the grip strength model, and the current discharge model. First, we overview the models and what requirements they are derived from. Then, we describe the testing methods used to verify these models. Finally, we analyze the results to show that they validate the design against functional requirements and overall success criteria.

A. Models

In this subsection, we present our theoretical engineering models.

A..1 Wind Loading Model

The wind loading model aims to guarantee that our structure can withstand the forces caused by the wind interacting with the balloon. This is derived from the functional requirement FR 8.0 that "the launching system shall function in 10 m/s sustained wind, with up to 20 m/s gusts". Thus, we begin by modeling the wind-balloon interaction.

First, consider the **static case**, where the windspeed is constant, and the **balloon does not accelerate**. Because the balloon has 0 acceleration, the force provided by the structure must be the same as the drag. Now, assuming the balloon is a rigid sphere with laminar flow informing the choice of coefficient of drag (.4), we may estimate the drag. These are conservative estimations meaning that the actual drag would be lower in the real world case as the balloon would likely fold over and not see the wind head on and turbulent flows would be likely as the balloon deforms and moves with the wind. The equation used for this calculation is:

$$D_{wind} = \frac{1}{2}\rho * V^2 * \pi * r^2 * C_D \tag{1}$$

$$D_{wind} = \frac{1}{2}(1.225kg/m^3) * (20m/s)^2 * \pi * (1m)^2 * (.4) = 308N \tag{2}$$

Next, the maximum load on the structure is considered in the case of **transient winds, where the balloon may accelerate**. According to [2], in 0.2s the wind speed may change from its sustained value to double its sustained value. In this case, that would be from sustained 10 m/s to gusts of 20 m/s. This time interval is used in the following analysis, although conservatively the wind interval from 0 to 20 is considered. The team begins by treating the balloon as a spring mass system, where the balloon is the mass, its connection to the gripper is the spring with constant k, and the structure is the where the spring attaches. The structure is assumed to be significantly stiffer than the balloon's neck, so that it may be considered static by comparison. In the model, the spring force is the force exerted on the wall (the structure), by the balloon's dynamics. The wind is the forcing function, $F(t)$. Thus, we may describe a 2nd order linear model as shown in Eq. 3. This model is for when the balloon is next to the tower, being blown out towards the side. That is, the balloon is not rotating, and its neck is being stretched. During winds, this configuration is expected, as this is observed for what happens when one user is performing the launch by hand.

$$
\begin{aligned}
m\ddot{x} + kx &= F(t) \\
x(\dot{0}) &= 0 \\
x(0) &= 0
\end{aligned} \tag{3}
$$

It is assumed that the wind quickly increases linearly from 0 m/s to 20 m/s, as described by the function $w(t)$ in Eq. 4. Then, using the previous method of calculating drag, the drag is calculated as a function of time, $D(t) = C_D \cdot S \cdot \rho w^2(t)/2$. The steady case gives values of C_D, S, and ρ.

$$
w(t) = \begin{cases} 0 & t \leq 0 \\ \frac{20}{0.2} \cdot t & 0 \leq t \leq 0.2 \\ 0 & 0.2 \leq t \end{cases} \tag{4}
$$

Thus, Eq. 3 may now be solved, either numerically, or through superposition of the homogeneous solutions of the form $\cos(\sqrt{k/mt})$ and $\sin(\sqrt{k/mt})$ with a particular solution corresponding to $F(t)$. However, Eq. 3 will be modified to include a damping term, as the balloon will have drag when it starts to move. Using the same drag as before, the damping is described as $B(\dot{x}) = C_D \cdot S \cdot \rho\dot{x}^2(t)/2$, giving the final ODE in Eq. 5.

$$
\begin{aligned}
m\ddot{x} + B(\dot{x}) + kx &= F(t) \\
x(\dot{0}) &= 0 \\
x(0) &= 0
\end{aligned} \tag{5}
$$

This equation is numerically solved, but first, we need to determine an equivalent spring stiffness, k, for our system. This is done by assuming a constant cross-sectional area, and Youngs' Modulus for the balloon neck. The team assumes that the balloon neck acts a spring for 6 centimeters ($L = 0.06m$), based on the physical reality of our loading configuration. The team assumes that the wind or setup configuration places the balloon body down-wind of the balloon neck in the gripper. In this situation, the balloon neck is purely in tension, pulling towards the release mechanism, and opposing any force from the wind. Videos of users holding the balloon show that this is a reasonable assumption. Thus, Eq. 6 may be used to calculate the extensive property of stiffness, from the balloon material's intensive Youngs' Modulus property, from [3]. For small deflections, the cross-sectional area of the neck will not change significantly, so the Poisson Effect's influence on the area is omitted for simplicity. This calculation is done by using the balloon's cross-sectional area from the undeformed configuration. This is an annulus, with an outer diameter of 5 cm, and a thickness of 2.5mm. The Youngs' Modulus for a similar material of rubber is $E = 0.1GPa$, from [4].

$$k = E \cdot \frac{A}{L} \tag{6}$$

Using the geometric and material properties previously described, $k = 6217.7N/m$. While this value may seem high, recall that this balloon neck is substantial in size, and that if it were made out of a stiffer material, the spring constant could still be over 1000 times larger. This stiffness describes how the balloon would respond if it is stretched along the length of its neck. Next to apply Eq. 6, the balloon's mass is 3.5 kg. Finally, Eq. 6 is solved numerically.

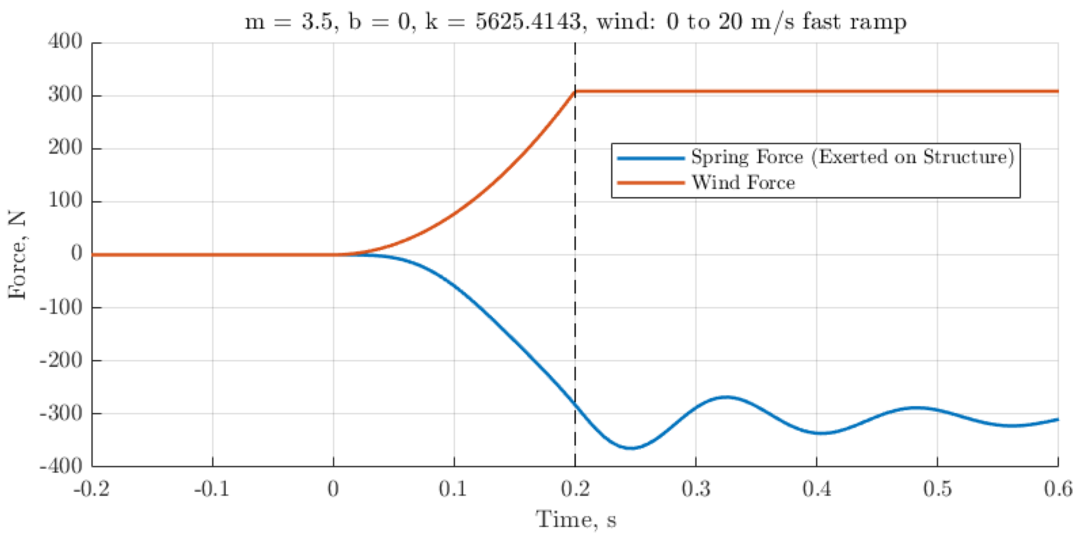

Figure 41 For a 0.2s wind velocity ramp from 0 to 20 m/s, the maximum force exerted on the structure is estimated as 365 N.

Fig. 41 shows the temporal response. The maximum force exerted on the force is calculated as 365 N. Note that as we take $\lim_{k\to\infty}$ or the wind-speed ramp time to ∞, the maximum force approaches our static ceiling of 308 N. Figure 42 shows the response to a slower velocity ramp, of 1 second.

However, these models assume that the wind goes from 0 to 20 m/s in the time that is originally defined for the wind to go from 10 m/s to 20 m/s. Thus, it is reasonable to use 0.4s for the wind to go from 0 to 20 m/s. Using the concept of the gust factor, this estimate is still conservative, compared to [2]. Similarly, the calculated k seems large, so for extra assurance, it will be systematically reduced by a factor of 10, as shown in Fig. 43.

Now, the team investigates the balloon's frequency dependence, given in Figure 44.

However, this linear ramp only weakly contains various frequency components in its frequency decomposition. Instead, the team will implement a sinusoidal ramp, which only has one frequency component. This will increase the excitation and show that balloon will not resonate with the wind. Figure 45 shows this behavior, with a sine forcing

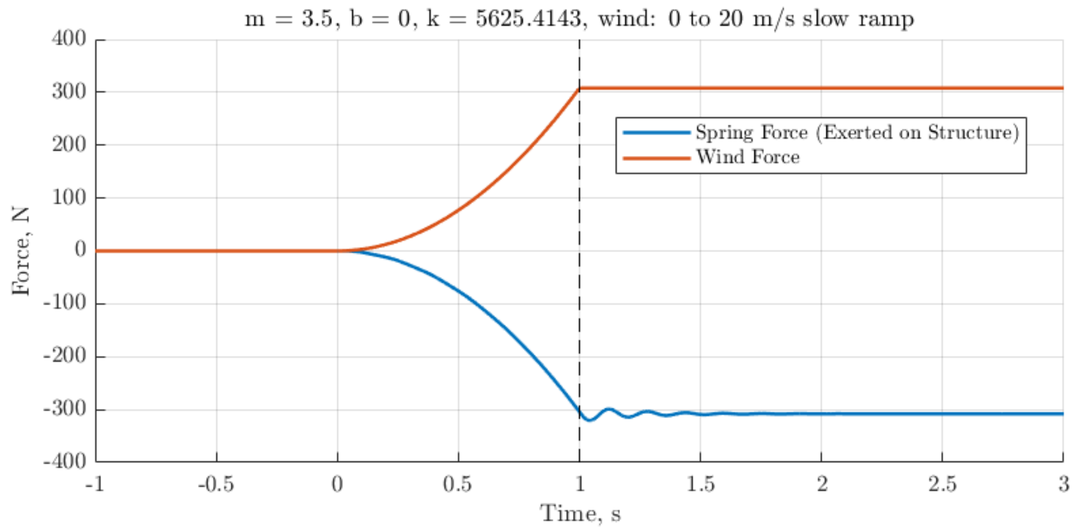

Figure 42 For a 1s wind velocity ramp from 0 to 20 m/s, the maximum force is significantly smaller than the faster ramp.

function. In fact, the frequency of the wind is too slow (too low) to excite the balloon. Thus, the ramp function provided more excitation, because of its higher frequency terms. In reality, the ramp frequency is even somewhat of an overestimate, and the team concludes that a maximum force of **365N** provides a ceiling for the worst case of dynamic wind loading. It is also worth noting that in both Fig. 44 and 45, as the duration of the wind increase approaches infinity (and the frequency of the increase approaches zero), the maximum force exerted on the structure approaches 308N, which is the calculation of the static force exerted on the structure. Clearly, this is as expected, supporting the team's method for dynamic loading analysis; further, the code used is included in the appendix.

With the force known at the top of structure the next step was ensuring that the components of the structure designed to provide stability could withstand the forces that would result from 20 m/s wind gusts potentially coming in any direction. This is shown in Figure 46. Two cases needed to be considered for this analysis for the strongest and weakest configurations of structure depending on the angle the wind is hitting it. The strongest configuration occurs with the wind directly coming along one of the supports (or at certain combinations of 2 supports opposing the wind as seen in the blue line on the plot in Figure 47) while the weakest configuration is when the wind is blowing at 30 degrees off of one of the supports. The calculation of sum of the moments (summing around base of the tower) for the strongest or 0 degree wind configuration is shown below:

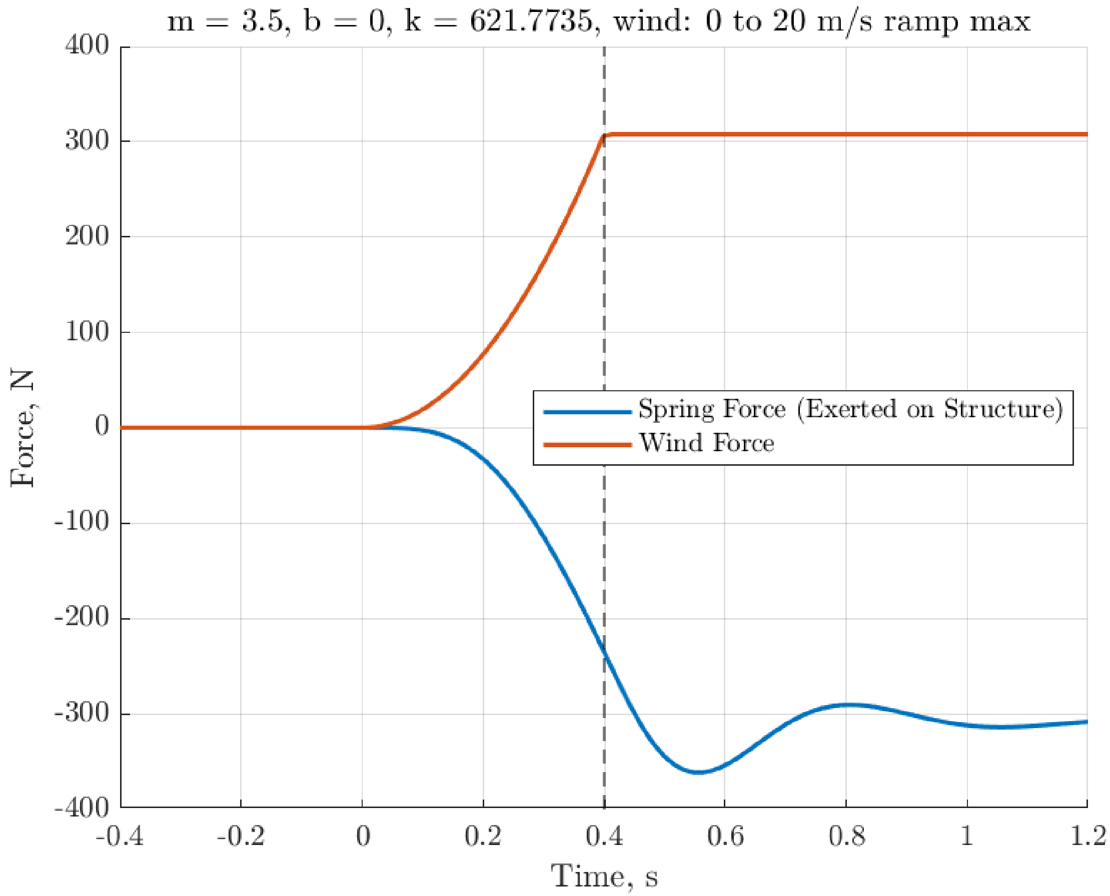

Figure 43 For a 0.4s wind velocity ramp from 0 to 20 m/s, the maximum force for a less stiff system is still within our upper 365 N force.

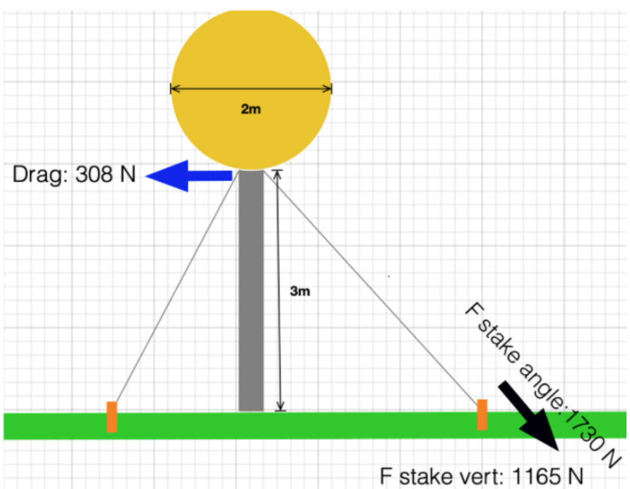

Figure 46 Structure Moments

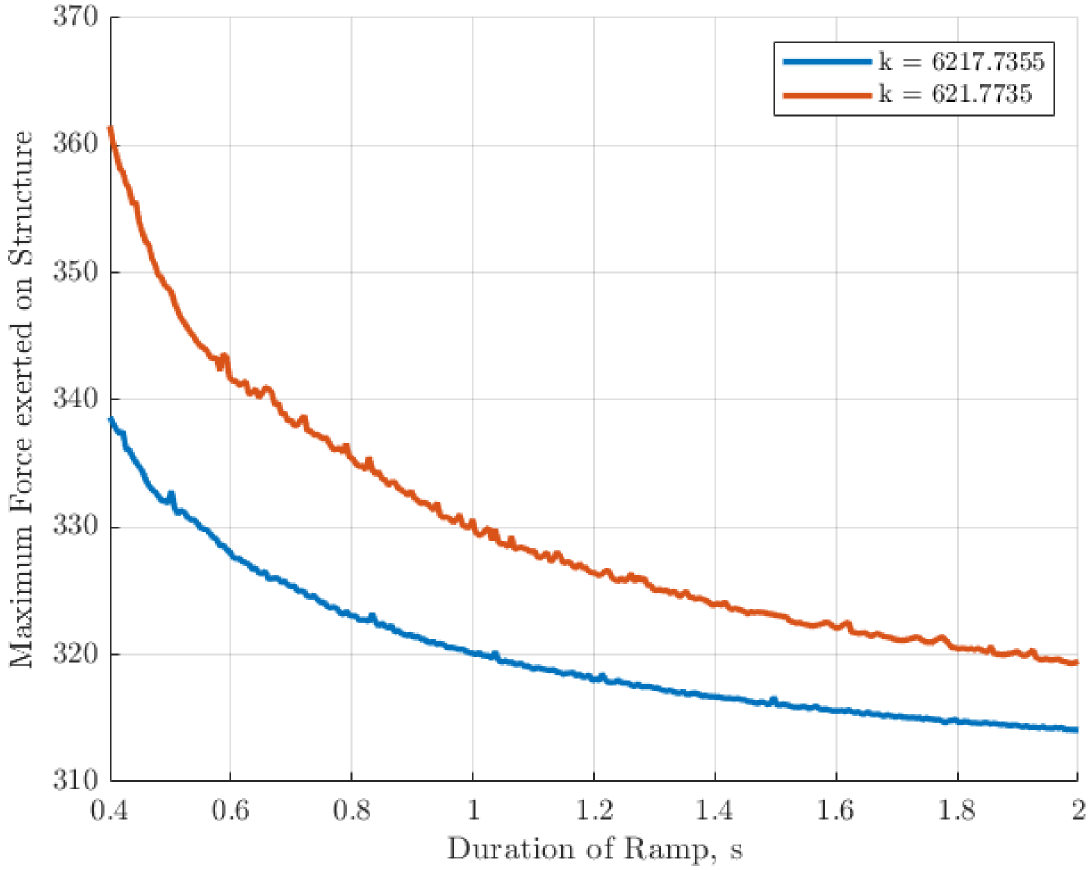

Figure 44 For a variety of time spans for wind velocity ramping from 0 to 20 m/s, the maximum force for the system does not exceed 365 N.

$$\Sigma M = D_{wind} * h_{tower} + F_{cable} sin(\theta) * h_{tower} = 0N \tag{7}$$

$$\Sigma M = 365N * 3m + F_{cable} sin(41.3) * 3m = 0N \tag{8}$$

$$F_{cable} = 553N \tag{9}$$

Turning towards the weakest configuration with the wind blowing at 30 degrees off one of the support cables, the force in the support cables is shown below:

$$F_{cable_x} = \frac{D_{wind}}{cos(30)} = 421.5N \tag{10}$$

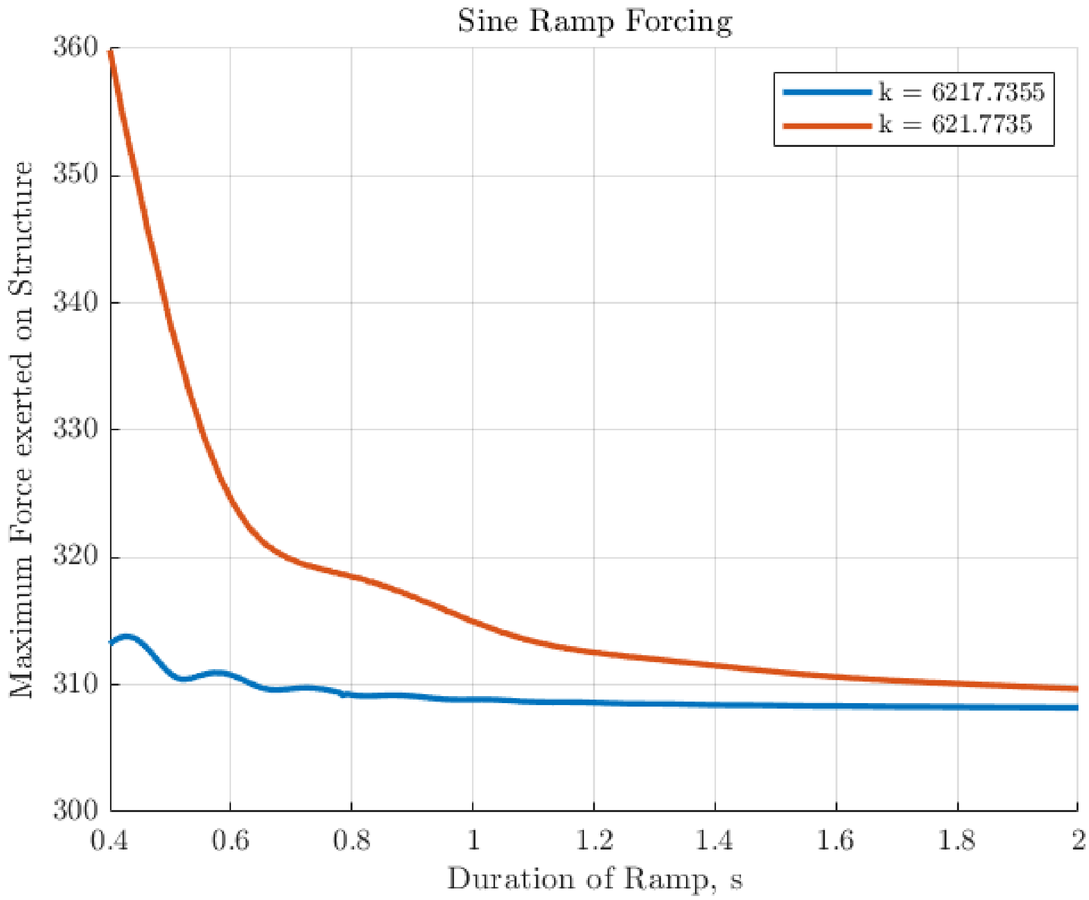

Figure 45 For a variety of time spans for wind velocity increasing from 0 to 20 m/s in a sinusoidal manner, the maximum force for the system does not exceed 365 N.

$$F_{cable} = \frac{F_{cable_x}}{sin(41.4)} = 638.6N \tag{11}$$

The tie downs and d-ring connection have a maximum tensile strength of 2225 N and the screw in stakes have a maximum strength at an angled pull (45 deg) of 1730 N so the 638N of maximum predicted force will not exceed the capability of the stability components. Therefore, the lowest factor of safety of this part of the structure is 2.7.

While the previous analysis verified the stability of the structure at it's strongest and weakest configurations with respect to wind direction, the team thought it prudent to model every possible angle the wind could hit the structure to ensure no "hidden" weaknesses were present. This analysis was done in Matlab imagining the wind coming in at every angle from 0 to 180 degrees to see how the moments it could resist would change. A top down view is shown in Figure 47 on the left with the results on the right. The maximum moment from the wind is shown in the orange line in Figure 47 at 1095N*m (3m*365N) with the blue line on top showing how much of a moment the structure can resist. As seen the blue line is always above the orange indicating that the structure is stable with wind coming in any direction, as the moment it can resist is always higher than the moment it will be subject to from the gusts. The factor of safety is 2.7.

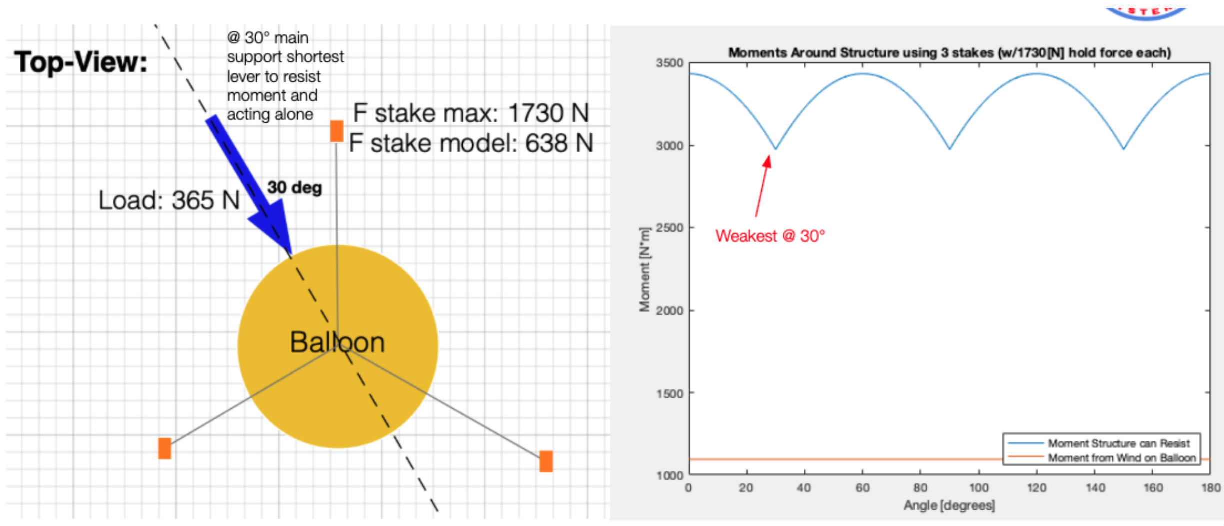

Figure 47 Structure Wind Direction Stability

Looking at the internal strength of the tower the weakest point concerned the plate joints where the 3 aluminum bars would be joined together. These would be in shear while the tower is raised before the drag is taken up by the support cables. Assuming the full shear on these components yielded factors of safety for the plates of 127 and the bolts at 44.

A..2 Grip Strength Model

The Grip Strength Model is used to verify there would be no premature release of the balloon from the release mechanism. The release mechanism holds the balloon securely to the structure using friction. This friction force is generated from the polyethylene foam blocks exerting a normal force on the balloon neck, due to the permanent electromagnet clasping the arms together. In order to find the friction force exerted between the foam blocks and the balloon neck some simplifications were made. The normal force of the foam block on the balloon neck is considered to be applied at a single point, in the center of the blocks. The swinging arms are also treated as a simple beam to perform a moment summation calculation as seen in Figure 48. The coefficient of friction used in our initial model is taken from that of latex rubber and polyethylene. The desired hold force to prevent premature release and counteract the wind force on the balloon is calculated to be 70.5 pounds force. The friction force calculated taking all assumptions into account is 267 pounds force. Therefor our model was expected to yield a factor of safety of 3.8.

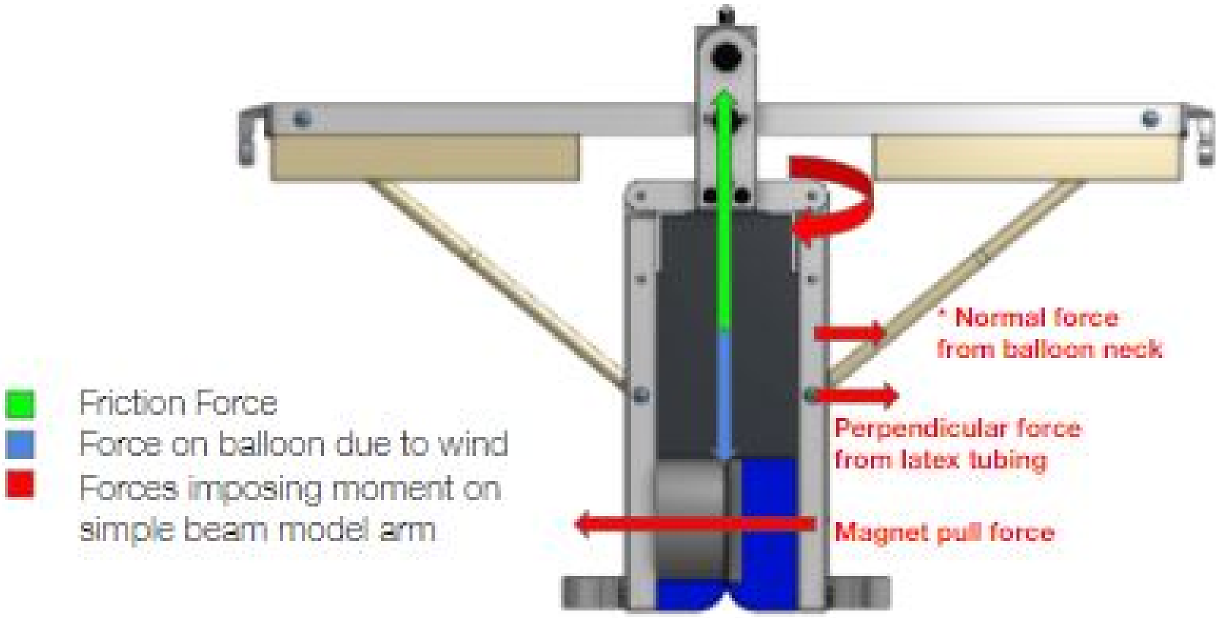

Figure 48 Modeled Friction Force

One factor overlooked in this model is the comprehensibility of the polyethylene foam. An assumption we unknowingly followed in the grip strength model, is that the foam would not compress. During initial testing using the foam blocks as the gripping surface of the release mechanism, the foam became worn down very quickly. This lead to a decreased hold force which allowed the rubber kitchen glove, which we used to simulate a balloon neck, to slip and make contact with the electromagnet. This proved to be problematic because the glove hitting the electromagnet eventually led to it tearing during one of our system tests. This presented the team with a new problem to solve. Brainstorming ideas to redesign the gripping surface included using wood blocks wrapped in latex, an eraser-type material, or a different kind of foam. Upon weighing the options, the group decided to order a sheet of 3/16 inch thick natural rubber. These were cut into rectangles in order to create a clean edge transition between the rubber pieces. The electromagnet/steel plate between the swinging arms PLA inserts were 3D printed. This new design resulted in our final design which can be seen in Figure 49. The natural rubber and PLA insert were much less compressible than the original design. Using the same equations as the initial model with a new coefficient of friction between latex and latex, the modeled friction force was then calculated to be 1,156 Newtons. Our required grip strength in Newtons was 365 Newtons which provides a factor of safety of 3.1.

Figure 49 Final Release Mechanism

This final design was then put through rigorous testing to validate the grip strength model. For the grip strength test, pull force was replicated using the original rubber kitchen glove attached to a nylon string. The glove was secured in the mechanism in the same way a balloon would be loaded. The opposite end of the string was attached to the measurement end of a spring scale. With safety glasses as a precautionary measure, the test administrator stood on the long back plate of the release mechanism and pulled up on the spring scale to simulate a wind force acting on the balloon. This procedure is shown in Figure 50.

Figure 50 Grip Strength Test

From ongoing iterations of the grip strength test, the average maximum force the release mechanism could hold is found to be 590 Newtons. This force provides a factor of safety of 1.61. It is important to note that winds that would create this force on the balloon are at speeds equivalent to tornado force winds. In testing it was also observed that the limiting factor of the overall grip strength was due to the load the latex would withstand rather than the mechanism itself. With this we would predict the balloon neck to tear from excessive wind force before the mechanism would lose grip on the neck.

Component	Voltage (V)	Current (A)	Power (Watts)	Time On (Minutes)	Charge (A-Hr)	Number of Launches
Receiver:						
Arduino Uno	12	0.2	2.4	5	0.017	
Electromagnet Gripper	12	3.25	39	5	0.271	
RF Board	5	0.01	0.05	5	0.001	
RF Rx	5	0.01	0.05	5	0.001	
1 Speaker with 12V Battery	12	0.01	0.12	0.5	0.000	
4 Channel Relay Shield for Arduino	12	0.01	90	5	0.001	
Rx Total					0.290	23.442
User:						
Remote Wireless Key Fob	3	0.04	0.12	0.5	0.000	630.000
Power:						
Rechargeable Battery Pack	12	6.8			6.800	23.442
CR2302 (Tx)	3	0.2			0.210	630.000

Figure 51 The power budget shows a margin of 22 additional launches.

B. Verification

Here, we examine the methods, procedures, and equipment used to verify our models through experimental testing. The critical project elements include ease of set-up/transport, stability in wind, internal structure strength, no balloon damage, no premature release of the balloon and hands free control of the release mechanism. Ease of set up/transport is verified by the final weight/dimension test, timed assembly test and the balloon loading test. Stability in wind is verified by the stake soil test and wind loading test. Internal structure strength is verified by the wind loading test. No balloon damage is verified by the balloon loading test, grip strength test and balloon launch test. No premature release of the balloon is verified by the grip strength test and balloon launching test. Finally, hands free release command will be verified by the current test, RF range test, and balloon launch test.

B..1 Weight/Dimension Test

The weight/dimension test involves weighing and measuring the packed system. This is completed using the full BDS system in its case along with a spring scale and tape measure. This test is aimed at verifying that the design elements related to packed size and weights of individual components matches the predicted numbers and satisfies the transportability requirements for the system.

Results gave a system weight of 33.2 lbs or 66 percent of the OSHA 50 lb limit and a length of 1.1m by .25 m by .25m. These results are within the customer's weight requirement and only 10 percent over the length. This verifies that the modeled weight for the system is accurate as it is within .2 lbs for what the team predicted. The modeled length is also accurate as the team was well aware that leaving the mast connections and kickstand attached when packed would increase the length requirement 10cm. The modeled height and width comes in .4cm lower than predicted as the team didn't not have a good estimate of how much cross sectional area would increase (of the packed system) once inside the travel case. Nevertheless, the height and weight match customer requirements.

B..2 Timed Assembly Test

The timed assembly test involves the complete packed system and a member of the BDS team. The packed system is taken to an open area and the BDS user is tasked with opening, unpacking and assembling the structure until it was standing and secure. This assembly is timed for each user. This test will verify whether the design elements intended to make the system easy, fast and intuitive to set up actually work as they were designed.

Results across 7 trials of BDS team members gave an average set up time of 10.03 minutes with a standard deviation of 6.26 minutes. Results are shown in Figure 52. This verifies that the BDS structure design elements aiming for fast set up are accurate and allow a single user to quickly set up the structure.

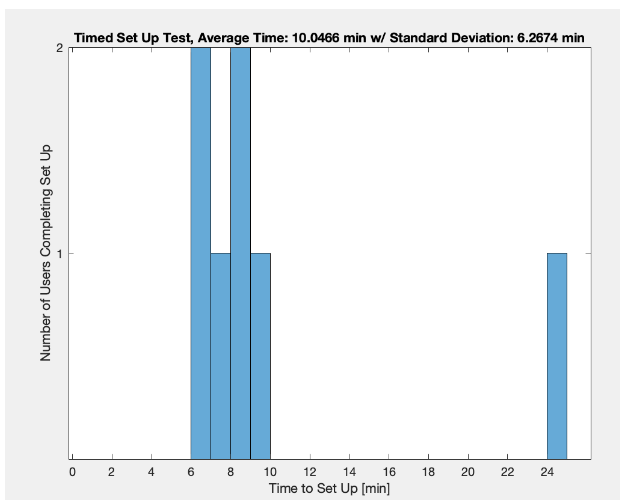

Figure 52 Timed Assembly Results

B..3 Wind Load Test

The wind load testing includes the BDS structure, ratcheting tie down straps, 2 spring scales and a ladder. The procedure involves setting up the structure next to a tree and connecting a ratcheting tie down between the tree and top of the structure. A spring scale is placed between the tree connected ratcheting tie down and the top of the structure to simulate wind loading. Once set up the structure is placed in two configurations, one with a support directly opposite the tree (the zero degree case) and one with the support at 30 degrees rotated away from the tree tie-down measure from looking in a top down view at the structure mast (the thirty degree case). In each case a team member climbs the ladder and begins increasing the load on the ratchet while another team member reads off the resulting load at the stakes. Tests are done both at a range of simulated wind loads and at the max expected wind load of 365N. The set up is shown in Figure 53. This test will verify the modeled maximum forces seen at the stakes from wind loading, that the modeled forces at the stakes across a range of wind loads are accurate and that the forces seen to internal components during maximum wind loading are not outside their limits. If verified the structure will be able to withstand launches in the maximum winds predicted.

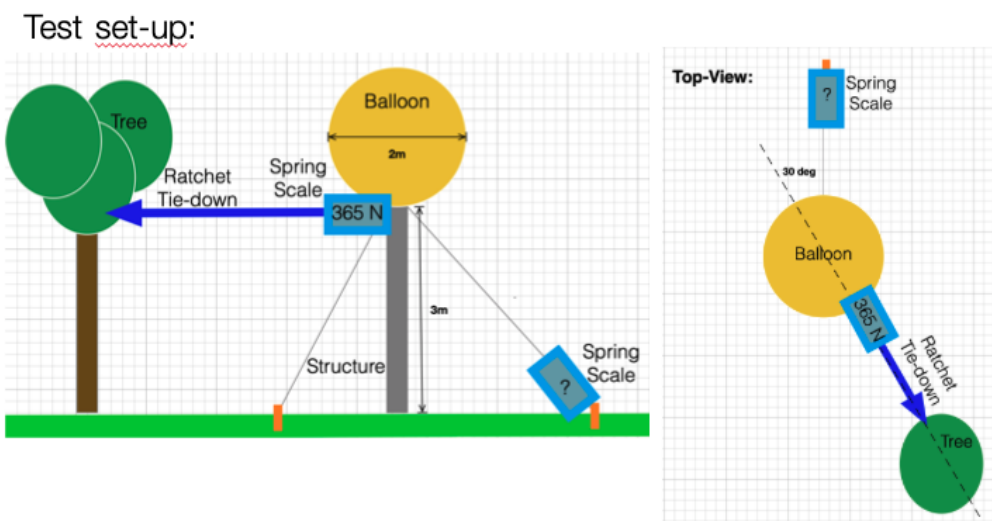

Figure 53 Wind Load Test Set Up

Results for the loading at the maximum expected wind load of 365 N are show in Figure 54. As can be see the orange line represents the max load the stakes can withstand provided by the manufacturer, the blue dots the modeled resulting stake load and the red dots the tested stake load. The modeled and tested values are very close (blue and red dots) and far below the maximum the stakes can withstand based on manufacturer data in both the zero and thirty degree cases. Higher loads are seen in the stakes in the thirty degree configuration and represent a factor of safety of 2.6 in this case when compared to the max manufacturer load ratings. Overall the max load at the stakes model is verified with this test.

Turning toward the results for a range of wind loading and how those were transmitted to the stakes, those results are seen in Figure 55. The results for the zero degree case are shown on the right and the results for the thirty degree case are shown on the left. The solid lines represent the modeled values and the dashed lines represent the best fit line of the data points shown with error bars in the plots. For the zero degree case the standard deviation is 10.5N and for the thirty degree case the standard deviation is 13.5 N. The shape of the model vs test data best fit lines in the zero degree case is nearly the same besides a 40N higher offset on the test data. This is due to the pre-tension in the cables present to keep

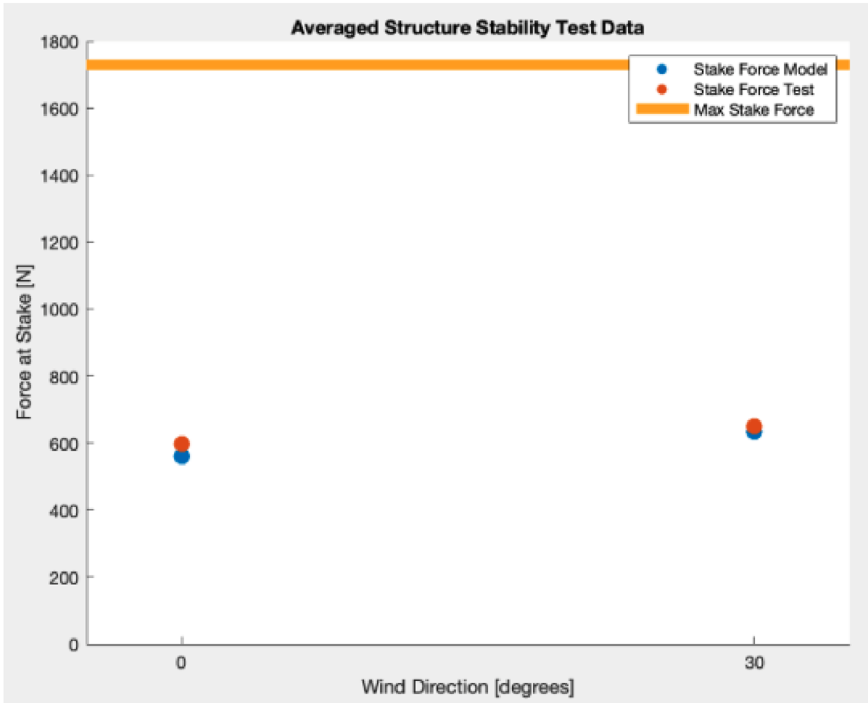

Figure 54 Wind Load - Max Load Results

the unloaded structure upright. This is not included in the model but has been measured empirically to be 40N as well. The thirty degree data also fits the model well but this offset is not present. This may be due to another support line taking up some of the load in this case as 30 degrees is right before another line begins taking up load as we rotate around the mast. If the line was actually at 31 or 32 degrees then another support would take some of the load which would reduce the tested values and appear like the tested best fit line shown. This situation is shown in Figure 56. The team plans to complete this test again with more precise angle measurements to remove the possibility of other lines taking up load. Overall, the range of wind load models are verified with the addition of the pre-load tension in the model.

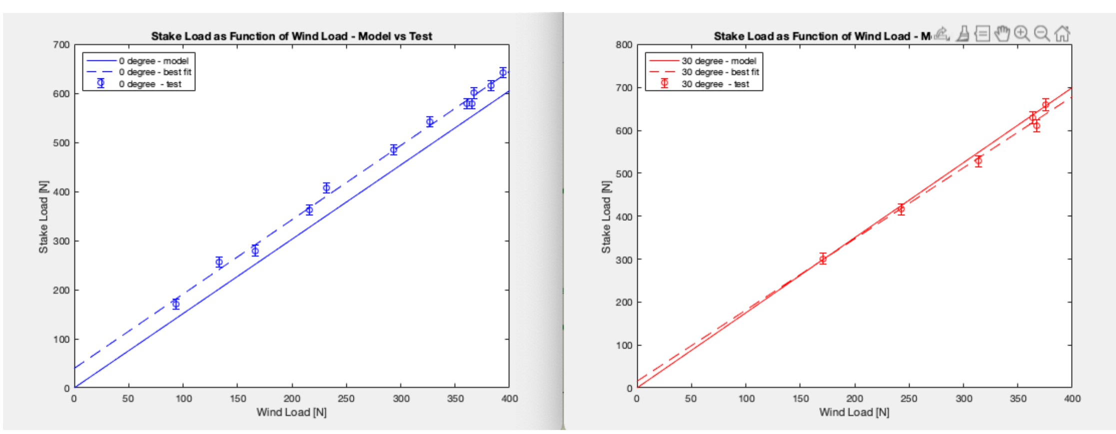

Figure 55 Wind Load - Range Load Results

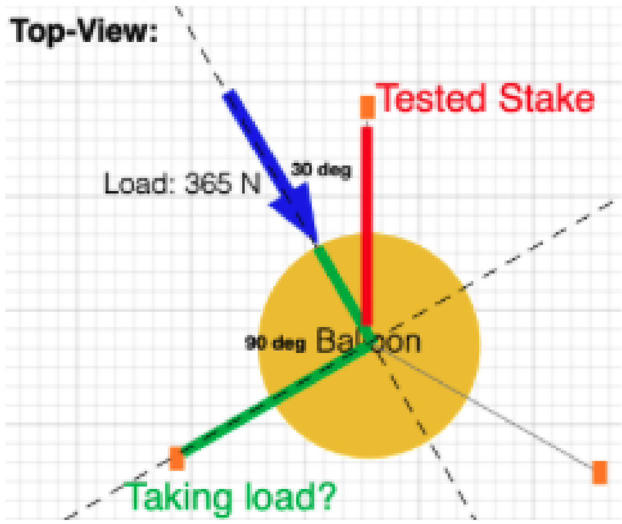

Figure 56 Wind Load - 30 deg No Offset?

B..4 Stake Soil Test

The stake soil test involves the screw in stakes, spring scale, ratcheting tie down and a soil moisture monitor. The process includes screwing a stake into the ground and attaching a spring scale and ratcheting tie down to a tree at 45 degrees. The soil moisture monitor is placed alongside the stake to verify the moisture in the ground. At this point the ratcheting tie down is used to increase the load on the stake until it begins to pull out. The maximum load and associated soil moisture is recorded. This test is completed in dry, medium and wet soil. Soil moisture is based on the rating from the Sonkir brand meter. The team has reached out to get a copy of how their scale aligns with actual percent soil mositure content and is still waiting for a response. However, the moisture monitor used will be included with the BDS so measurements made during future launches can be compared agsint the forthcoming results. This test will verify the stake manufacturer ratings for hold force and determine additional ground conditions feasible for high wind launches.

Results are shown in Figure 57. The soil moisture is shown across the horizontal axis and stake hold forces is shown on the vertical axis. The orange line is the manufacturer load rating and the black line is the maximum load required by the HYFLITS team based on launching in 20 m/s winds. Results show that the screw in stakes perform better than the manufacturer claims in dry conditions (above 1730N) but fall off as moisture increases to around 1450N. Nevertheless, even in wetter conditions the hold force is still sufficient for the HYFLITS high wind launching needs based on the max stake hold force required as given by the wind loading model.

B..5 Balloon Loading Test

The balloon loading test requires the assembled structure resting on the kickstand with a helium filled Kaymont high altitude balloon and latex gloves. The test involves one user opening the release mechanism, loading the balloon and

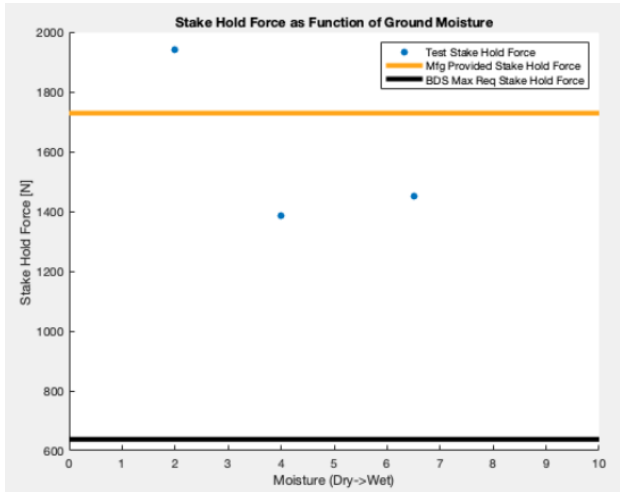

Figure 57 Stake Soil Test Results

then closing the release mechanism as if preparing to launch. This test will verify whether the modeled forces required for a single user to open and load the balloon are reasonable for use and how intuitive the loading process is generally.

Across 10 trials the balloon was successfully loaded by a single user with no balloon damage or premature release occurring. Additionally the release mechanism feature of removing one side of the surgical tubing for easier clamping of the balloon was found to not be necessary and the team was able to omit that step. However, the trials did make clear the importance of altering users to the necessity of having the balloon venting valve point away from the structure to avoid it catching on release mechanism after it begin flying away. Comparing to the loading model, this model is perhaps too stringent in requiring easier closure of the release mechanism as an adult hand can easily close the clasp with both pieces of surgical tubing attached. The release timing model (time for balloon neck to rise clear of mechanism during launch) however is verified as users who mistakenly loaded the balloon with the venting valve facing the structure found it was likely to catch during subsequent release tests.

B..6 Grip Strength Test

The grip strength test includes the release mechanism, a rubber dishwashing glove to simulate the balloon, rope, a spring scale and weights. The rubber glove has weights tied to the cuff area via the rope with the hand area of the glove being placed and locked inside the release mechanism. The user then lifts the differing weights with the release mechanism verifying the grip strength between the glove material and release mechanism arms.

Results over 25 trials found an average hold force of 590N, representing a factor of safety of 1.61. The grip strength model predicted a maximum strength of 1156N. It is important to note that this test was not done to failure as the rope/glove failed before the release mechanism lost grip. Therefore the modeled max strength at 1156N cannot be verified directly. However, tested values being significantly above the maximum required hold force of 365N indicates that testing verifies that the system will still exceed requirements for holding the balloon in high winds.

B..7 Current Discharge

To test our current discharge model, we developed a simulated user, that would actuate the system like the real user, measure current and voltage, and repeat the process. Thus, we could form a voltage-current relationship for the battery, in addition to knowing when the voltage is too low for the system to operate. This discharge profile additionally allows for us to implement a low power warning to the user. We added the INA219 current sensor to our system. Additionally, we implemented a Raspberry Pi to entirely automate the testing process. This was done after initial testing suggested that our battery had much more charge than we previously predicted. This additional microcontroller allowed for us to keep all of our launch code exactly the same, providing the most realistic imitation of real launches. The Raspberry Pi served as both the user, and the sensor system. For a given launch, the Raspberry Pi would set the button pin of the arduino to a *high* state. This imitates the user pressing the wireless transmitter button, and the signal being transmitted to the receiver (arduino) system, arming the system. After a delay, the Raspberry would set the pin high again, corresponding to the *launch* command. The Raspberry Pi then uses the INA219 current sensor to measure the voltage across the battery and adds one to the launch total. When this process is repeated, we may generate a plot of *number of launches* vs. *Battery voltage*.

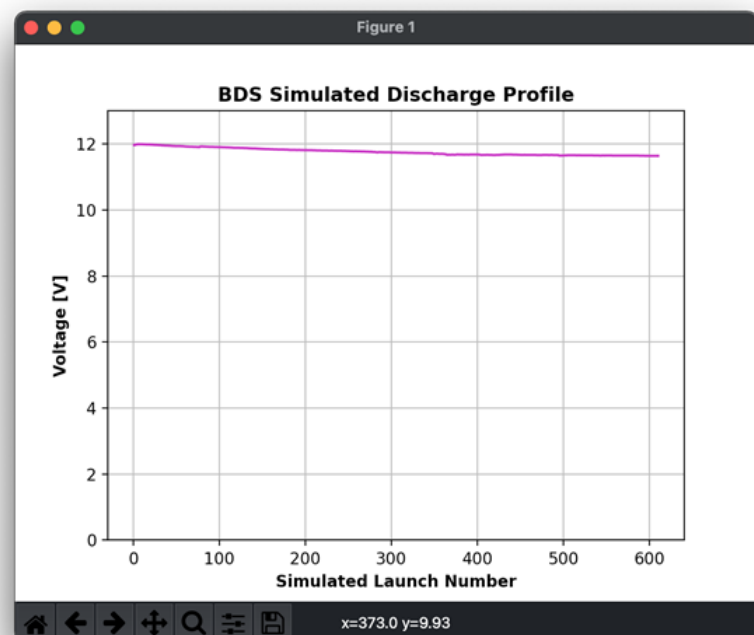

Figure 58 Caption

Further, from our previous full system testing, we found that user would open the gripper for only about 5-10 seconds, significantly less than our predicted 5 minutes from our power budget. With this adjustment, our power budget would be predicting 60 times the number of launches (1200 launches). The testing results are given by Fig. 58. This much greater factor of safety is again due to our previous overestimate of how long it would take a user to load the system.

B..8 RF Range Test

The RF range test requires the full BDS system along with a tape measure. After setting up the structure and turning on the command and control unit, a team member with the remote walks away from the structure in 1 m intervals, testing at each point whether the command and control box could receive the signal, indicated with the arm tone. This test will verify the manufacturer's stated range for the transmitter purchased.

Results give an average range of 17.6m with a standard deviation of 3.8m across 21 trials with results shown in the histogram in Figure 59. This is significantly lower than the manufacturer stated range of 40m. The teams models require a range of 19.8 m (using the HYFLITS 20m length tether) as measured from the users feet to the base of the BDS at the high end assuming the payload tether is being held with no slack. Therefore the test results indicate that it could be difficult to achieve reliable activation of the release mechanism from the full 19.8 m away, as the average is only 17.6m. However, in terms of usability and function of the actual system, it is unlikely this 2m of reduced distance will have a large impact on the balloon being sufficiently aloft to avoid the payload hitting the ground, as it is still 90 percent of the full distance away.

B..9 Balloon Launch Test

The balloon launch test includs the full BDS system, a helium filled Kaymont high altitude balloon, dummy payload and balloon tether. After setting up the structure, the balloon is filled with helium and then tethered to one of the structure ground stakes to avoid losing the expensive balloon and helium and allow for multiple trials. The test is carried out from loading the balloon, raising the structure and finally having the user walk away with payload and remote to release the tethered balloon. Data is collected regarding the ease of balloon release and safety of the balloon during the process. This test will verify whether the set up and launch process works as intended and whether any issues have been missed during a full launch. Specifically the modeled rise time of the venting valve moving away from the release mechanism, the most likely catching scenario, will be verified with this test.

10 trials have so far been conducted with the above test with everything except the payload release in high winds. In the low to moderate winds tested in so far, no balloon damage has occurred, no premature release of the balloon has happened, the balloon has not gotten snagged or tangled and hands free release has worked via the remote each time. This verifies the team's design elements of removing any sharp edges and adding foam near the top of the structure to

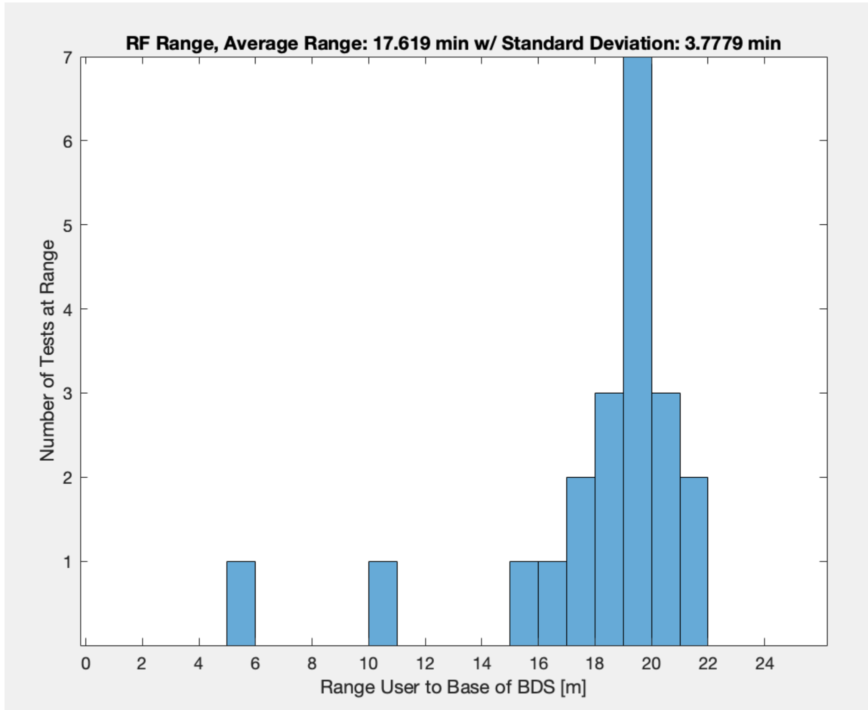

Figure 59 RF Range Test Results

prevent any damage to the balloon. Furthermore this also verifies the command and control system in that the arm and then release command functions as intended and releases the balloon when desired.

Looking specifically at the chance of the balloon/valve snagging during release, the time from the release to the venting valve passing the bottom of the release mechanism is modeled to be .27 seconds. This model is based on the rate of ascent of the balloon with no wind present (most likely scenario for catching). Analysis of videos during the release indicate this is accurate as it takes on average .3 seconds for the venting valve to clear the release mechanism with 11 percent error. Therefore the release timing model is verified.

C. Validation

In this subsection, we show how the data from the previous section validates the design against functional requirements and overall project success criteria. The functional requirements are given again below for reference:

FR 1.0 "One person shall be able to assemble/disassemble the BDS with no tools."

FR 2.0 "The assembly/disassembly shall takes less than 5 minutes to complete."

FR 3.0 "The structure shall collapse into a carrying bag of 1 m length and 25 cm diameter maximum."

FR 4.0 "The payload shall not hit the ground during setup or deployment."

FR 5.0 "If needed, capability to launch two balloons within one second of each other."

FR 6.0 "The BDS shall be made of heat resistant materials and have no sharp edges which might damage the balloon."

FR 7.0 "The BDS shall function in 10 m/s sustained wind with up to 20 m/s gusts."

FR 8.0 "Communication between the BDS and the release button shall be hands-free."

FR 9.0 "All systems shall be powered by battery."

C..1 Weight/Dimension Test

The weight and dimension test aims to validate FR 3.0 "The structure shall collapse into a carrying bag of 1 m length and 25 cm diameter maximum." The height and width dimensions have been met exactly and the length of the case is 10 percent over the 1m requirement. The components that put the length above are the connecting plates between the 8020 bars of the structure and the kickstand. Both of these are removable and would allow the length requirement to be met exactly. However, this extra step would increase set up time substantially and impinge on FR 2.0. Therefore the team decided to trade the slightly increased length for much quicker set up. It is worth noting that the extra length does not prevent the packed system from fitting into a small car trunk or back seat so the usability it not impacted. This meets level I success for portability being below 50 lbs and fitting in a compact car trunk.

C..2 Timed Assembly Test

The timed assembly test looks to validate FR 2.0 "The assembly/disassembly shall takes less than 5 minutes to complete." This was not met as the average assembly time was just over 10 minutes and the absolute fastest time was just over 6 minutes. Nevertheless, as our results showed, with practice HYFLITS team members could approach the 6 minute set up time. As mentioned before this achieves level I success for portability.

C..3 Wind Load Test

Wind load testing validated FR 7.0 "The BDS shall function in 10 m/s sustained wind with up to 20 m/s gusts.". The results of testing indicate that the system is highly stable in 20 m/s or higher winds coming in any direction. Furthermore the internal strength of the structure was validated in the wind load testing as no bending or failures of components occurred. This represents Level III success for balloon security.

C..4 Stake Soil Test

Stake soil testing further validated FR 7.0 "The BDS shall function in 10 m/s sustained wind with up to 20 m/s gusts." as the stake hold force was shown to be sufficient to launch in 20m/s winds when launching from a variety clay or soil surfaces with varying moisture contents. Again this aids the achievement of level III success for balloon security.

C..5 Balloon Loading Test

The balloon loading test attempts to validate FR 4.0 "The payload shall not hit the ground during setup or deployment." and does validate FR 6.0 "The BDS shall be made of heat resistant materials and have no sharp edges which might damage the balloon.". Ensuring that the payload does not hit the ground during loading was difficult to test as it is up to the user to use care with the payload while the balloon is being loaded. With that said the system is designed with d-rings at the top of the structure which the payload can be clipped to during loading to avoid damage and ground contact. The team is still awaiting high wind launch conditions to further ensure that when actually launched the height of the structure will be sufficient to avoid the payload swinging into the ground. Turning to FR 6.0 regarding ensuring that the system does not pose a risk to the balloon, the balloon loading test validates this. All stakes are away from the balloon and all edges near the balloon have been smoothed or covered in foam. The success of these design elements is evidenced by the fact that over 10 trials loading the balloon the balloon sustained no damage from the system.

C..6 Grip Strength Test

The grip strength test validates FR 7.0 "The BDS shall function in 10 m/s sustained wind with up to 20 m/s gusts." As mention previously, the average grip of the release mechanism is 590 N which is a factor of safety of 1.6 over the required 365 N of max force required in 20 m/s winds. This achieves level III success for balloon security in that the balloon will not be released prematurely by the system in high winds.

C..7 Current Discharge

We seek to validate the functional requirements FR 8.0 and FR 9.0 with this test. As a reminder, FR 8.0 and FR 9.0 require the deployment is hands-free and that the launcher/release mechanism is battery powered, respectively. The battery power requirement is necessary for the hands-free deployment, as our system is wireless, and both the transmitter and receiver must be properly powered for the system to be actuated at all. Thus, ensuring that the system is properly battery powered is necessary for our system to be hands-free. From Fig. 58, we see that our battery sustains hundreds of launches on one charge. Clearly, for a single launch on a single charge, the battery will not fail. A factor of safety of at least 600 is exceptionally high, which additionally accounts for user error and unforeseen circumstances. Thus, FR 9.0 is completely validated by this test, which in turn supports part of FR 8.0.

Beyond the functional requirements, this also provides extra safety and peace of mind to the user. The user may accidentally leave the system on overnight, and the system is likely to still function. Further, this allows for us to implement a low power warning to the user, a nice feature that is much beyond the requirements set forth by the customer. In sum, the testing reveals that our power system has substantially exceeded expectations.

C..8 RF Range Test

RF range testing helps to validate both FR 8.0 "Communication between the BDS and the release button shall be hands-free." and FR 5.0 "If needed, capability to launch two balloons within one second of each other." The RF range test results thus far indicate that the user waist mounted and elbow operated remote functions at an average of 17.6m away from the launching structure. This validates hands free release requirements at that distance, which, as previously mentioned, is sufficient for enough height to be attained by the balloon for the payload to avoid hitting the ground. Results for the two balloon launch are pending.

C..9 Balloon Launch Test

The balloon launch test is designed to test multiple requirements including FR 4.0 "The payload shall not hit the ground during setup or deployment.", FR 6.0 "The BDS shall be made of heat resistant materials and have no sharp edges which might damage the balloon.", FR 7.0 "The BDS shall function in 10 m/s sustained wind with up to 20 m/s gusts.", and FR 8.0 "Communication between the BDS and the release button shall be hands-free." The nature of the tests so far has validated FR 6.0 relating to no balloon damage and FR 8.0 regarding hands free release commands but until testing can be completed in higher winds with the dummy payload, FR 4.0 and FR 7.0 relating to the payload not hitting the ground and the entire system working in actual high winds is yet to be fully validated.

VI. Risk Assessment and Mitigation

Authors: Kyler Stirewalt

The majority of BDS's risks come from constant wind and strong gusts. When outside and ready to launch, the balloon often bumps into the BDS repeatedly with the wind; which is the risk that was deemed most probable. To minimize the chance of balloon damage, all exposed edges of the structure were chamfered and foam was secured around the release mechanism. Later during testing, thanks to customer feedback, a foam cap was attached to the top of the structure.

Ensuring that the balloon does not prematurely release in strong gusts is a risk that consumed a lot of testing time. As soon as the release mechanism was manufactured, we began to test the grip strength using a latex kitchen glove. The tests revealed a new way in which the release mechanism might fail. Instead of forcing the magnet open, the glove would slip out of the arms along the perpendicular axis. These tests prompted us to find a foam with a higher coefficient of friction with latex. After searching, the most optimal material available was attached to the arms and now the BDS can hold balloons in 80 mph winds (category 1 hurricane speeds).

Once all the subsystems were finished and the integration phase started, the transceiver range was much less than predicted. By chance, we discovered that if the release button is held in a certain orientation, the range is maxed; like pointing a remote directly at a TV. Instead of reworking the release button, to boost signal strength we drilled a hole in the electronics box on the structure for the antenna to poke out. Another risk that became evident during integration is that the stakes don't hold as well in wet ground. The stakes never came out, but would form donut-like rings of dirt as their straps were fully tightened and they moved slightly. To fix this, much larger stakes were bought and the BDS can launch in any soft ground except sand.

Two risks which were originally deemed remote happened more often than expected. In the design phase, we were aware that the venting valve might catch on the release mechanism before it could fully open. The catching seemed improbable, but it caught a few times in the first tests. We soon realized that the balloon must be loaded directionally (which is clarified in our user manual). We started loading balloons with the venting valve facing outwards, away from the hinge of the release mechanism, and it has not caught in this configuration. The other risk is more user-related. Early in the project we predicted that all the tethers from the payload and the stakes might get tangled in the wind. They did tangle, but not from the wind. Until the user loads a few balloons, it can be confusing to make sure all the connectors are in the right place lest the user have to take the structure down to correct it. To aid in this, we added a color coding scheme to our connectors.

Throughout the project development, few of the predicted risks posed a serious threat to the success of the project. Amidst the pandemic, only one of our packages was delayed and it did not impact us even though we deemed that risk probable. Due in part to a simple design without moving parts, the risks inherent to the BDS have been minimized and their consequences are low severity.

VII. Project Planning

Authors: Jake McGrath

A. Overview

B. Organizational Chart

The structure of the Balloon Deployment System team was very deliberate, but also follows naturally from the subsystem breakdown of the project. As a team of ten, the work that we need to complete was too large to be accomplished efficiently as one working team, so we divided the team into working groups no larger than five. The main sub teams of the Balloon Deployment System team are as follows:

- Management Team
- Structures Team

- Release Mechanism Team
- Command and Control Team
- Testing and Risk Team
- Systems Engineering Team

The division and creation of these teams naturally followed from the three main subsystems of the project as well as the needs that had arisen to address testing procedures and risk assessment towards the end of the semester. Since we are limited to ten people, almost every team member contributes to multiple teams. We do not anticipate the organizational structure to change in second semester; each subsystem team will be responsible for their own manufacturing, the testing/risk team will handle testing for each subsystem, and the systems engineering team will coordinate the interfacing of each subsystem.

Additionally, the division of the team into subsystems allows one subsystem team to red-team the design and work products of another team, affording us with an easily accessible set of eyes.

The Balloon Deployment System Team organizational chart is found in figure 62, and highlights each position followed by the team member. One important thing to note is that everyone on the team has a leadership role or is in charge of a portion of the project. While this might seem like a "too many cooks in the kitchen" situation, this has worked quite well for our project. There are numerous leadership theories and readings that point to the importance of team members having skin in the game. The most notable of which, "Skin in the Game" by Nassim Nicholas Taleb [11] suggests that team members having personal stake in the project is essential for productivity, fairness, and output. On the balloon deployment system team, each team member wasn't merely assigned to a portion of the project; everyone had the opportunity to choose their sub team based on their personal interests and goals. As the semester progressed and we were presented with a need for more team roles, we selected them in the same manner. Additionally, we all participated in a survey gauging what we hoped to be involved with more, what we wanted our titles to be, and where we hoped to grow so that the team structure can be continually adjusted to help meet everyone's personal goals in addition to the team's.

Next, the Balloon Deployment System team is aligned directly with the complexity model of leadership and organizations, discussed in Komives and Dugan's "Contemporary leadership Theories" [10]. The goal of complexity leadership is to foster system-level adaptive outcomes such as increased innovation, learning, and creativity while also acknowledging the context in which leadership occurs, suggesting that organizational structures and decision making must be adaptive and responsive and that influences on this are neither wholly individual nor systemic. In practice, we accomplish this by being divided into small teams, or nodes, which are a part of a larger system. Each node is able to work autonomously to an extent within the confines of the project and in the name of satisfying customer requirements. Every node does not have to work with every other one, so collaboration is made naturally where appropriate while also ensuring information is transparent and available to all of the rest of the team members. The challenge of designing the

BDS is too large to be handled at a team wide level, so each node handles a portion of the problem independently, and it is the job of systems engineer and project manager to make appropriate connections where they have not already made. If done correctly, this organizational style works well on its own, provided the project manager continually contextualizes work and provides clear markers for each team to follow. Complexity leadership removes much of the overhead cost of having team meetings, and ensures that everyone is working on the most necessary part of the project to their team. This style of leadership has become very popular amongst tech companies due to its flexibility and developmental agility–we have shown that it also applies well to our senior projects team.

C. Work Breakdown Structure

The work breakdown structure of the project followed naturally from the division of subsystems; a chart depicting the BDS work breakdown structure can be found in figure 63. Each subsystem is independent for the most part and can stand alone sans their bolt on interface.

The support structure can be viewed as both a stabilizing component and a vertical component. In this case, the stabilizing component consists of the screw in stakes and adjustable straps. No assembly is required for the stabilization portion. The vertical structure consists of three 80/20 aluminum bars that are bolted together to raise the balloon to three meters. The stabilization component interfaces with the vertical structure through the use of carabiners; no special assembly or tools are required.

The release mechanism cannot be subdivided any further and acts as a single unit that interfaces with the balloon. This component requires some rudimentary machining, but for the most part can be assembled with commonly available tools, fasteners and adhesives.

Next, the command and control system consists of the receiving module that commands the release mechanism and the sending module that the user wears on their waist. The command and control system has been deliberately designed to reduce the number of soldiered or terminated connections in order to increase reliability and decrease manufacturing effort. This is primarily accomplished through the use of Arduino shields to connect the Arduino to the relay and receiver. The only wiring work we will have to perform is terminating ends; the team happens to have eight years of commercial and residential electrical experience so this should not be an issue. These components are stored in an off the shelf box and secured using common adhesives like double sided tape.

Finally, in addition to the individual subsystems, the release mechanism and command and control system interfaces with the structure via a bolted connection. The command and control system interfaces with the release mechanism via terminated connections.

D. Work Plan

One of the best parts of this project from a planning perspective is the independent nature of each subsystem. Each subsystem can stand alone in terms of manufacturing, assembly, and testing, which affords us tremendous flexibility. Each sub team is working on a portion of the project in parallel and sub teams communicate and collaborate where necessary.

We have painstaking developed a Gantt chart for the second semester using a project management software called ClickUp. This software does not allow us to easily export the Gantt chart or display it in a method that would fit in the document, so a copy of the chart can be found HERE. The chart is organized into four main phases: material procurement, assembly, testing, and customer turnover. Since the project is inherently parallelized, each task has dependence on previous tasks denoted by arrows. The software will not let us start on or complete a task until all of the dependencies have been satisfied. The project has two main milestones: the subsystem assembly completion and the system preliminary assembly, scheduled to take place in early February and early March respectively. This allows for the entire month of February to be dedicated to testing and iterating our subsystem and the entirety of March to be dedicated to testing and refining the structure and procedures.

E. Cost Plan

The BDS was particularly easy to budget thanks to our customer requirements. One of the most critical design aspects was that the system had to cost less than $1,000 to manufacture. We kept this in mind throughout the duration of the design process and only considered designs which met this specification. As a result, we had a very large margin which allowed us to put careful budgeting on the back burner. We had initially predicted that the cost of the BDS would be $991.58, as shown in figure 60, leaving us an astounding $4,000 left in our development budget. At the end of development, we were able to reduce the cost of the BDS by 4% for a final price tag of $950.06. One of the areas which we did not carefully plan was testing; we had initially predicted a test cost of just over $100. We had completely neglected purchasing balloons and helium which ended up costing more than the entire structure. We knew that this would be a consideration, but we did not think it worth to plan for given our large overhead. Had this not been the case, however, we would have completely blown our budget and made the customer very unhappy. In the future, especially in industry, considering every aspect of the project is paramount as such large margins are very uncommon. In the end, we ended up using just over half of our $5,000 development budget.

F. Test Plan

The modularity of the BDS made testing very efficient. The majority of the tests we conducted throughout the semester were subsystem tests which did not rely on the entire product being complete. The key tests are noted by

Subsystem	Predicted Cost	Actual Cost	Percent Change
System	$ 991.58	$ 950.06	-4.19%
Command and Control	$ 184.63	$ 207.52	12.40%
Release Mechanism	$ 306.42	$ 258.35	-15.69%
Structures	$ 409.88	$ 434.20	5.93%
Testing	$ 104.97	$ 1,239.39	1080.71%
Budget Total	$ 991.58	$ 2,545.31	156.69%

Figure 60 BDS Initial Cost Versus Actual Cost

flags at the top of the chart in figure 61; with the exception of the full system test, every other test could be thoroughly completed as manufacturing was completed. This allowed us to very quickly find and patch any holes in our design and allowed each sub team to make full use of their time together. Our only test which required special accommodations was the balloon loading test. The HYFLITS team typically performs launches from the hazardous test cell which is where the helium and filling equipment is located. Access to this area did not require any reservations or scheduling and was completely empty each time we used it. We were able to complete all of our tests on time with the exception of the wind test; we were able to perform some testing in limited gusts, but we have yet to experience a day with 20 m/s gusts. We do not anticipate that the BDS will fail this test as we have taken special care to design each component to be balloon safe with large factors of safety. At present, our average grip strength test shows that fragile latex can be safely in forces created by 35 m/s winds, 1.75 times higher than our maximum design criteria.

VIII. Lessons Learned

Authors: Jake McGrath

Over the course of the semester, the Balloon Deployment System team learned many valuable lessons, especially with respect to customer communication. At the beginning of the semester, we met with our customer to discuss his needs for the project; after this we did not communicate as much as we should have. At many crucial steps of the project, like defining our levels of success, design, and trade studies, we simply guessed what our customer would want based off of our initial meetings rather than simply asking for clarification. There were several parts of our project that were either ill-defined or resulted in more work than was necessary.

A specific example of ill defined criteria is how we defined set up time and portability in our levels of success. Initially, we had said that level three setup time was five minutes and portability was one meter. At the end of the

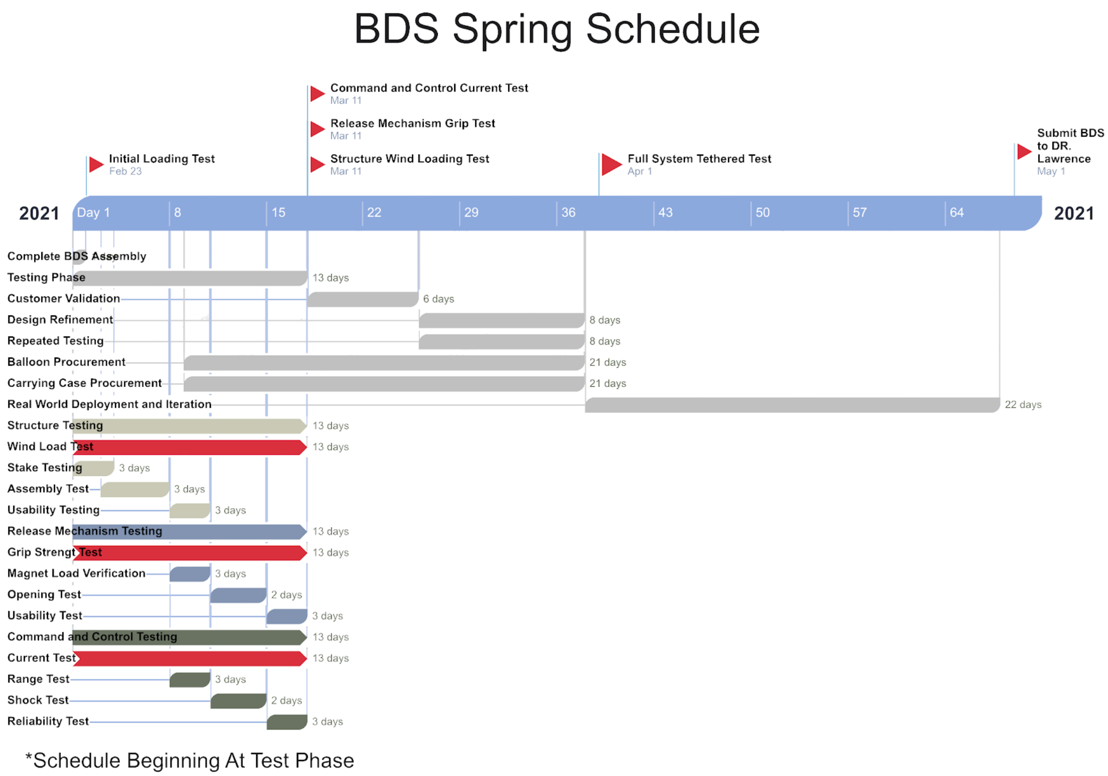

Figure 61 BDS Test Gantt Chart: Structures Test Denoted by Tan, Release Mechanism Test Denoted by Blue, Command and Control Denoted by Red

semester, our system ended up being 1.1 meters long and we were able to set up the system in six minutes at the fastest. Functionally, these differences did not effect the success of our project, yet we were only able to meet level two success according to our own definitions. In hindsight, it would have been better to define our levels in terms of ranges rather than discrete numbers.

Furthermore, more frequent communication during the design process would have resulted in less iteration late in the semester. We quickly learned that on of the most important parts of the systems engineering process is well thought out trade studies. Even though we conducted our studies according to what we thought was best at the time, we now know that the weights we assigned to each of our categories was very wrong. This caused us to chose a design that was ultimately too cumbersome for the customer and required a complete redesign. Looking back, had we changed our weights to more accurately reflect what what the customer needed, not what we thought best, our final design would have manifested itself much sooner. Overall, these mistakes taught us valuable lessons about customer communications and the systems engineering process. Senior projects is a great place to fail; we are given a real world, low consequence environment where it's safe to learn and make mistakes without dire consequences. A mistake here won't cost us our jobs and we are constantly given feedback from very experienced PAB members. The mistakes we made over the semester ultimately made each of us better engineers.

IX. Individual Report Contributions

Authors:

- Aufa Amirullah: Final Design, Manufacturing
- Peter Hurst: Manufacturing, Verification and Validation
- Austin Konnath: Manufacturing, Verification and Validation
- Jake Joseph McGrath: Project Planning, Lessons Learned
- Grant Norman: Final Design, Verification and Validation
- Patrick Paluszek: Final Design
- Jack Soltys: Project Objectives and Functional Requirements
- Kyler Stirewalt: Project Objectives and Functional Requirements, Risk Assessment and Mitigation
- Sebastian Urrunaga: Final Design,Project Objectives and Functional Requirements
- Chenshuo Yang: Manufacturing

X. Appendix

A. Instructions

The following instructions is the assembly manual.

1) Open bag
2) Assemble Tower
3) Thread in base steak
4) Lay staking template on the ground
5) Screw in stakes at the 3 corners of template
6) Deploy kickstand on mast
7) Kickstand should be over the center of the template
8) Clip Tie Down Support to D-Ring on Top of Mast
9) Clip opposite ends of tie-down to stakes
10) Ensure Tie-Down Cams Loosed to Knot
11) Turn on Electronics Box
    - Flip power switch to on
    - If release mechanism arms need to be separated, flip override switch
    - Clip remote to user for elbow activation

12) Load Balloon in Release Mechanism
    - Ensure release mechanism open
    - Place balloon in release mechanism with foam valve tube facing away from mast and balloon neck clamped as close to base of balloon as possible
    - Push release mechanism arms together until magnet clicks closed
13) Raise mast and place base stake at center of template
14) Tighten tie-downs, ensuring mast straight
15) Walk back with payload, begin launch command
    - While holding payload, hit green button with elbow once to arm (listen for beeping to indicate armed)
    - Press again to release balloon
    - Prepare to release payload once balloon overhead

B. Arduino Code

The following code is the Arduino code for Command and Control system which contains several functions that support BDS system to have a wireless-link command and hands-free operation.

```
/*The following 4 pin definitions,correspond to 4 buttons on the remote control(The
    telecontroller is Remote Wireless Keynob 315MHz(SKU:FIT0355))*/
int D1 = 8;    //The digital output pin 1 of decoder chip(SC2272)
int D2 = 9;    //The digital output pin 2 of decoder chip(SC2272)
int D3 = 10;   //The digital output pin 3 of decoder chip(SC2272)
int D4 = A5;   //The digital output pin 4 of decoder chip(SC2272)
int power = A4; // The digital output to deactivate pin
int buzzer = 13;   //Receiving indicator

/* For the Relays*/
byte relayPin[4] = {4, 7, 8, 12}; // initialize relay pin
int gripper_relay = relayPin[2];
int buzzer_relay = relayPin[3];

/* For the Launch Arm Sequence*/
int counter = 1;
```

```
/* For battery check*/
int beeped = 0; // Check if the speaker has beeped
int level;

void setup()
{
  Serial.begin(9600);

  /*The four pins order below correspond to the 4 buttons on the remote control.*/
  pinMode(D4, INPUT);  //Initialized to input pin, in order to read the level of the output
      pins from the decoding chip
  pinMode(D2, INPUT);
  pinMode(D1, INPUT);
  pinMode(D3, INPUT);
  pinMode(power, OUTPUT);
  pinMode(gripper_relay, OUTPUT);
  pinMode(buzzer_relay, OUTPUT);

  pinMode(power, INPUT); // For battery check

  digitalWrite(buzzer, LOW);
  digitalWrite(power, HIGH);
}

void loop()
{
  if (digitalRead(D4) == HIGH) {
    if (counter % 2 != 0) {
      delay(1);
      beep(10, 250, 500);
      deactivateFob(250);
```

```
    } else {
      delay(1);
      beep(3, 2000, 500);
      deactivateGripper(10000);
      deactivateFob(250);
    }
    counter = counter + 1;
  }
}

void deactivateFob(int duration) {
  digitalWrite(power, LOW);
  delay(duration);
  digitalWrite(power, HIGH);
}

void deactivateGripper(int duration) {
  digitalWrite(gripper_relay, HIGH);
  delay(duration);
  digitalWrite(gripper_relay, LOW);
}

void beep(int nbeeps, int del, int start_del)
{
  delay(start_del);
  for (int i = 0; i < nbeeps; i++) {
    digitalWrite(buzzer_relay, HIGH);
    delay(del);
    digitalWrite(buzzer_relay, LOW);
    delay(del);
  }
}
```

C. MATLAB Code

Included below is the MATLAB code for the dynamic modeling of the balloon, with varying wind forces. Please review the section outlining the logic behind this code first. Note that the file *s.m* is a class for running various of these simulations efficiently, with easy potential for further changes. The file *Dynamic_stiffness.m* is the main driver script, configuring the parameters for *s.m*. Finally, *derivative_fcn.m* describes the dynamics of the system. This is the implementation of the equations of motion.

C..1 Dynamic_stiffness.m

```
clc; clear all; close all;
set(groot,'defaulttextinterpreter','latex');
set(groot, 'defaultAxesTickLabelInterpreter','latex');
set(groot, 'defaultLegendInterpreter','latex');

% Sources:
% https://www.azom.com/properties.aspx?ArticleID=920
% https://en.wikipedia.org/wiki/Stiffness
% https://en.wikipedia.org/wiki/Torsion_constant
% https://www.engineeringtoolbox.com/modulus-rigidity-d_946.html

% Thickness of latex
th = 0.00225; % m
th2 = 0.0025;
% Top of release mech to bottom of sphere of balloon.
l = 6 / 100; % m
% Mass of balloon
m = 3.6; % kg
% Damping coefficient, not related to drag.
b = 0;
t_disturb = 0.2;
% vprofile = '0 to 20 m/s fast ramp';
% sve = 'fastramp';
%
```

```
% ss = s(l,th,b,t_disturb,vprofile,sve); % 0.2 s ramp
% slow = s(l,th,b,1,'0 to 20 m/s slow ramp','slowramp'); % 1 second ramp
%
% tss = s(l,th2,b,t_disturb,'0 to 20 m/s ramp max thickness','thicker'); % 0.2 s ramp

t_disturb = t_disturb*2;

% smallerk = s(l*10,th2,0,t_disturb,'0 to 20 m/s ramp max ','dyn_sim-factor10');

ts = 0.4 + linspace(1.6, 19.6,300);
maxF = zeros(size(ts));
maxFs = zeros(size(ts));
maxF2 = zeros(size(ts));
for i=1:length(ts)
    si = s(l,th2,0,ts(i),'0 to 20 m/s sine ramp','dyn_simLOOP');
    si2 = s(10*l,th2,0,ts(i),'0 to 20 m/s sine ramp','dyn_simLOOP');
%     s_sine =  s(10*l,th2,0,ts(i),'0 to 20 m/s sine ramp','dyn_sine');
%     maxFs(i) = s_sine.maxf;
    maxF(i) = si.maxf;
    maxF2(i) = si2.maxf;
end


figure();
hold on;
plot(ts,maxF,'linewidth',2);
plot(ts,maxF2,'linewidth',2);
% plot(ts,maxFs,'linewidth',2);
xlabel('Duration of Ramp, s');
ylabel('Maximum Force exerted on Structure');
legend(['k = ',num2str(si.k)],['k = ',num2str(si2.k)]);
title('Sine Ramp Forcing')
```

```
grid on;

s_sine =  s(l,th2,0,t_disturb,'0 to 20 m/s sine ramp','dyn_sine');
maxsF = s_sine.maxf;



% smallerk = s(l*4,th2,0,t_disturb*2,'0 to 20 m/s ramp max ','dyn_sim-t04_l4');
%
% smallerrk = s(l*10,th2,0,0.075027058162628*5,'0 to 20 m/s ramp max ','dyn_sim-t04_l6');
% smallerrk = s(l*10,th2,0,0.075027058162628*5-0.2,'0 to 20 m/s ramp max ','dyn_sim-t04_l6')
    ;
% smallerrk = s(l*10,th2,0,0.075027058162628*5-0.1,'0 to 20 m/s ramp max ','dyn_sim-t04_l6')
    ;

% damped = s(l*4,th2,0,t_disturb*2,'0 to 20 m/s ramp max ','dyn_sim-t04_l4');
% damped = s(l*4,th2,0,t_disturb*2,'0 to 20 m/s ramp max ','dyn_sim-t04_l4');
% damped = s(l*4,th2,0.1,t_disturb*2,'0 to 20 m/s ramp max ','damp'); % 0.2 s ramp
```

C..2 s.m

```
classdef s
    %UNTITLED2 Summary of this class goes here
    %   Detailed explanation goes here

    properties
        k
        C
        b
        m
        th
        l
        t_disturb
        v
        vprofile
```

```
        sve
%         maxf
    end
    properties (Dependent)
      maxf
    end

    methods
        function obj = s(l,th,b,t_disturb,vprofile,sve)
            %UNTITLED2 Construct an instance of this class
            %   Detailed explanation goes here
            % Constant Parameters

            D = 5 / 100; % m
            E = 0.001 * 10^9; % Pa
            A = pi/4 * (D^2 - (D-2*th)^2); % m^2
            k = E*A/l; % N/m
            C = 0.77; % C_d * S /2 (for 308N drag)
            m = 3.5; % Double check!

            obj.k = k;
            obj.C = C;
            obj.b = b;
            obj.m = m;
            obj.th = th;
            obj.l = l;
            obj.t_disturb = t_disturb;
%             obj.maxf = 0;

            % Defualt is linear ramp. Modify this by using obj.v = @(t) ...
            % after constructiong
%             obj.v = @(t) 20/obj.t_disturb .* t .* (0 < t & t< t_disturb) + 20 .*(t_disturb
```

```
    <= t);
%             v_m = @(t) 20/obj.t_disturb .* t;
            v_m = @(t) 20*sin(t* (pi/2)/t_disturb);
            obj = setv(obj,v_m);
            % For plotting
            obj.vprofile = vprofile;
            obj.sve = sve;
%             disp([sve,' max force:']);
%             obj.maxf = run(obj);
        end

        function obj = setv(obj,v_m)
            v = @(t) v_m(t).*(t>0 & t<obj.t_disturb) + v_m(obj.t_disturb) .*(obj.t_disturb
                <= t);
            obj.v = v;
        end

        function [maxf] = get.maxf(obj)
            %METHOD1 Summary of this method goes here
            %   Detailed explanation goes here
            y0 = [0; 0];
            tspan = [-1*obj.t_disturb 3*obj.t_disturb];
            [t,y] = ode45(@(t,y) derivative_fcn(obj,y,t), tspan, y0);
            Fspg = -obj.k*y(:,2);
            Fwind = obj.C * obj.v(t).^2;



%             save = 0;
% %             save = 1; % Toggle for automatic saving
%             figure();
%             hold on;
%             plot(t,Fspg,'linewidth',1.5);
```

```
%             plot(t,Fwind,'linewidth',1.5);
%             ys = ylim;
%             plot([obj.t_disturb obj.t_disturb],ys,'--k');
%             grid on;
%             legend('Spring Force (Exerted on Structure)','Wind Force','location','best');
%             tle = ['m = ',num2str(obj.m),', b = ', num2str(obj.b), ', k = ', num2str(obj.k
    ),...
%                 ',  wind: ',obj.vprofile];
%             title(tle);
%             xlabel('Time, s');
%             ylabel('Force, N');
%             if save == 1
%                 saveas(gcf,[obj.sve,'.png']);
%             end
%             disp(max(abs(Fspg)));
            maxf = max(abs(Fspg));
        end
    end
end
```

C..3 derivative_fcn.m

```
function [yp, Fspg] = derivative_fcn(s,y,t)
    r = y(1);
    x = y(2);
    xp = r;
    rp = ((s.v(t)-r)^2 * s.C - s.k*x - s.b*r)/s.m;
    yp(1) = rp;
    yp(2) = xp;
    yp = yp';
end
```

C..4 Moment Model and Test Data Plotting

```
%% ASEN 4018 model - Main
```

```matlab
%Author: Peter Hurst
%Date: September, 2020
%% housekeeping
clc;
clear all;
close all;
%% Constants
Mtn_Hard=267;
m=3.68; %kg
Coleman_10=400; %[N]
Orange_small_angle=1730; %[N]
Orange_small_vert=1165; %[N] 1165
Test_stake_load=552;
F_stake=Orange_small_angle;% [N] Coleman Stakes: 400N, Orange screw stakes 1730N
n_stakes=3;
V_inf=20; % [m/s]
Cd=.4; %drag coefficient
rho=1.225; % [kg/m^3]
d=2; %balloon diameter in [m]
%D=(1/2)*rho*V_inf^2*(pi/4)*d^2*Cd; %drag in [N]
D=365; %365
truss_height=3; %truss height, sum moment around truss base [m]
balloon_height=3; %[m]
tot_mom_resist=balloon_height*D;
L_cable=4;% [m]
L_cable_h=sqrt(L_cable^2-truss_height^2);
Num_stake_cable=1; %number of stakes at each cable end
theta_tot=2*pi;
theta=2*pi/n_stakes;
thetas=zeros(360,n_stakes);
for k=1:n_stakes
```

```
    thetas(1,k)=thetas(1,k)+(k-1)*360/n_stakes;
end
for i=1:length(thetas)
    for j=1:n_stakes
        thetas(i+1,j)=thetas(i,j)+1;
    end
end
for i=1:length(thetas)
    for j=1:n_stakes
        if thetas(i,j)>360
            thetas(i,j)=thetas(i,j)-360;
        end
    end
end
M_0=zeros(length(thetas),n_stakes);
%M_0(:,1)=thetas(:,1);
for j=1:n_stakes
    for i=1:length(thetas)
        x=sind(thetas(i,j))*L_cable_h;
        y=cosd(thetas(i,j))*L_cable_h;
        z=truss_height;
        u=[x y -z];
        u_AB=u/norm(u);
        r=[0 0 truss_height];
        Fu=F_stake*Num_stake_cable*u_AB;
        m_x=cross(r,Fu);
        if m_x(1)<0
            M_0(i,j)=m_x(1); %this just puts only positive values into the M_0 matrix so
                they aren't negated on the other side of the structure
        end
    end
end
```

```
total_mom=zeros(length(M_0),1);
for i=1:length(M_0)
    total_mom(i,1)=sum(M_0(i,1:n_stakes));
end



figure(1)
tot_mom_resists=tot_mom_resist.* ones(length(thetas),1);
plot(thetas(:,1),-1*total_mom);
hold on
plot(thetas(:,1),tot_mom_resists);
title(['Moments Around Structure using ',num2str(n_stakes),' stakes (w/',num2str(F_stake), '
    [N] hold force each)']);
xlabel('Angle [degrees]');
ylabel('Moment [N*m]');
xlim([0 180]);
hold on
scatter([0,30],[(-1+.065)*total_mom(1),(-1+.075)*total_mom(31)],'filled','red'); %test data
hold on
% scatter(thetas(31,1),-1.075*total_mom(31),'filled'); %test data
ylim([0 3700]);
legend('Moment Structure can Resist','Moment from Wind on Balloon','Moment Tested', '
    Location', 'southeast');
hold off




%%checks
theta_check=22;
x_check=sind(theta_check)*L_cable_h;
y_check=cosd(theta_check)*L_cable_h;
z_check=truss_height;
```

```
u_check=[x_check y_check -z_check];
u_AB_check=u_check/norm(u_check);
r_check=[0 0 truss_height];
Fu_check=F_stake*Num_stake_cable*u_AB_check;
m_x_check=cross(r_check,Fu_check);

F_hand=[2.64*sind(theta_check) 2.64*cosd(theta_check) -3];
F=F_stake*F_hand/norm(F_hand);
mom_hand=cross([0 0 3],F);
```

```
%% dynamic loading
% k=1000; %N/m with 20 rubber bands
% c=0;
% [t,y] = ode45(@(t,y) springmassdamper(t,y,m,c,k), [0 .5], [0 0]);
% figure
% plot(t,y(:,1),'r','LineWidth',1);
% hold on;
% plot(t,y(:,2),'k','LineWidth',1);
% legend('Velocity', 'Displacement');
% xlabel('Time (s)');
% ylabel('Displacement (m)');
%       title('Spring-Mass-Damper');
```

```
%% stake forces testing
% theta_stakes=[0:1:30];
% T_y=L_cable_h*cosd(theta_stakes);
% Fc_top=D./cosd(theta_stakes); %changed from /
% Fc_stake=Fc_top/sind(atand(L_cable_h/truss_height));
%
% F_stake_hold=F_stake.*ones(length(theta_stakes));
%
% figure(2)
% plot(theta_stakes,F_stake_hold);
```

```
% hold on
% plot(theta_stakes,Fc_stake);
% title('Force on Up Wind Stake w/Wind Direction Change');
% xlabel('Wind Direction [degrees]');
% ylabel('Force at Stake [N]');
% legend('Stake Force Applied','Stake Force Max Hold');
% hold off
%
% % hold on
% % scatter([0,30],[450,480]);
%
 %testing data
test_data=[0 0 0 30 30 30; 546 579 555 605 637 658;580 616 601 660 630 660]';
err_p=(test_data(:,2)-test_data(:,3))./test_data(:,3);
error=test_data(:,2)-test_data(:,3);
mean_error_0=mean(error(1:3));
mean_error_30=mean(error(4:6));
% test_data(:,2)=test_data(:,2)./cosd(test_data(:,1));
% test_data=sortrows(test_data,1);
figure
%errorbar([0 30],[mean(test_data(1:3,2)) mean(test_data(4:6,2))], [mean_error_0,
    mean_error_30],'vertical','o');
scatter([0 30],[mean(test_data(1:3,2)),mean(test_data(4:6,2))],90,'filled');
hold on
scatter([0 30],[mean(test_data(1:3,3)),mean(test_data(4:6,3))],90,'filled');
hold on
plot ([-5 35], [1730 1730],'color',[1, 0.647, 0.0980],'LineWidth',6);
% figure
% scatter(test_data(:,1),test_data(:,2));
% hold on
% scatter(test_data(:,1),test_data(:,3));
title('Averaged Structure Stability Test Data');
```

```
xlabel('Wind Direction [degrees]');
ylabel('Force at Stake [N]');
legend('Stake Force Model','Stake Force Test', 'Max Stake Force','Location','northeast');
xlim([-5 35]);
ylim([0 1800]);
xticks([0 30]);
```

```
%% Wind Load Testing
%error test data
wind_load_0=[361 383 367 94 166 216 294 365 133 232 327 394];
stake_test_0=[580 616 601 171 280 363 485 580 257 407 542 643];
wind_load_0_range=linspace(0,400,10);
model_load_0=wind_load_0_range/(sind(41.3));



%uncertainty calculation 0 degree calculation
sums_0=0;
p_0=polyfit(wind_load_0,stake_test_0,1);
B_0=p_0(1);
A_0=p_0(2);
for i=1:length(stake_test_0)
    sums_0=sums_0+(stake_test_0(i)-A_0-B_0*wind_load_0(i))^2;
end
sigma_y_0=sqrt((1/(length(stake_test_0)-2))*sums_0);
best_fit_0=A_0+B_0*wind_load_0_range;

wind_load_30=[364 376 171 243 314 367 416];
stake_test_30=[630 660 301 416 528 611 695];
wind_load_30_range=linspace(0,400,10);
model_load_30=wind_load_0_range/cosd(30)/(sind(41.3));

%uncertainty calculation 30 degree configuration
```

```
sums_30=0;
p_30=polyfit(wind_load_30,stake_test_30,1);
B_30=p_30(1);
A_30=p_30(2);
for i=1:length(stake_test_30)
    sums_30=sums_30+(stake_test_30(i)-A_30-B_30*wind_load_30(i))^2;
end
sigma_y_30=sqrt((1/(length(stake_test_30)-2))*sums_30);
best_fit_30=A_30+B_30*wind_load_30_range;

%plotting
figure
plot(wind_load_0_range,model_load_0, 'b');
hold on
plot(wind_load_0_range,best_fit_0,'Color','b','LineStyle','--');
hold on
errorbar(wind_load_0,stake_test_0,[sigma_y_0 sigma_y_0 sigma_y_0 sigma_y_0 sigma_y_0
    sigma_y_0 sigma_y_0 sigma_y_0 sigma_y_0 sigma_y_0 sigma_y_0 sigma_y_0],'vertical','o','
    Color','b');
xlabel('Wind Load [N]');
ylabel('Stake Load [N]');
title('Stake Load as Function of Wind Load - Model vs Test');
legend('0 degree - model','0 degree - best fit', '0 degree  - test', 'Location', 'northwest'
    );

figure
plot(wind_load_30_range,model_load_30, 'r');
hold on
plot(wind_load_30_range,best_fit_30,'Color','r','LineStyle','--');
hold on
errorbar(wind_load_30,stake_test_30,[sigma_y_30 sigma_y_30 sigma_y_30 sigma_y_30 sigma_y_30
    sigma_y_30 sigma_y_30],'vertical','o','Color','r');
```

```
xlabel('Wind Load [N]');
ylabel('Stake Load [N]');
title('Stake Load as Function of Wind Load - Model vs Test');
%legend('0 degree - model','0 degree - best fit', '0 degree  - test', '30 degree - model
    ','30 degree - best fit','30 degree  - test','Location', 'northwest');
legend('30 degree - model','30 degree - best fit','30 degree  - test','Location', 'northwest
    ');
xlim([0 400]);
ylim([0 800]);
```

```
%% set up time data
times=[9.08 8.5 24 8.78 7.666 6.25 6.05];
num_time_testers=length(times);
avg_time=mean(times);
std_times=std(times);
edges=[1:25];
figure
histogram(times, edges);
xticks([0 2 4 6 8 10 12 14 16 18 20 22 24]);
yticks([1 2 3 4 5 ]);
xlabel('Time to Set Up [min]');
ylabel('Number of Users Completing Set Up');
title(['Timed Set Up Test, Average Time: ' num2str(avg_time) ' min w/ Standard Deviation: '
    num2str(std_times) ' min']);
```

```
%% soil data
moisture=[2 4 6.5];
soil_force=[1942 1386 1452];

figure
scatter(moisture, soil_force, 'filled');
hold on
```

```
plot ([0 10], [1730 1730],'color',[1, 0.647, 0.0980],'LineWidth',4);

hold on

plot ([0 10], [638 638],'color','k','LineWidth',4);

title('Stake Hold Force as Function of Ground Moisture');

xlabel('Moisture (Dry->Wet)');

ylabel('Stake Hold Force [N]');

xlim([0 10]);

legend('Test Stake Hold Force', 'Mfg Provided Stake Hold Force', 'BDS Max Req Stake Hold
    Force');
```

D. Organizational Chart

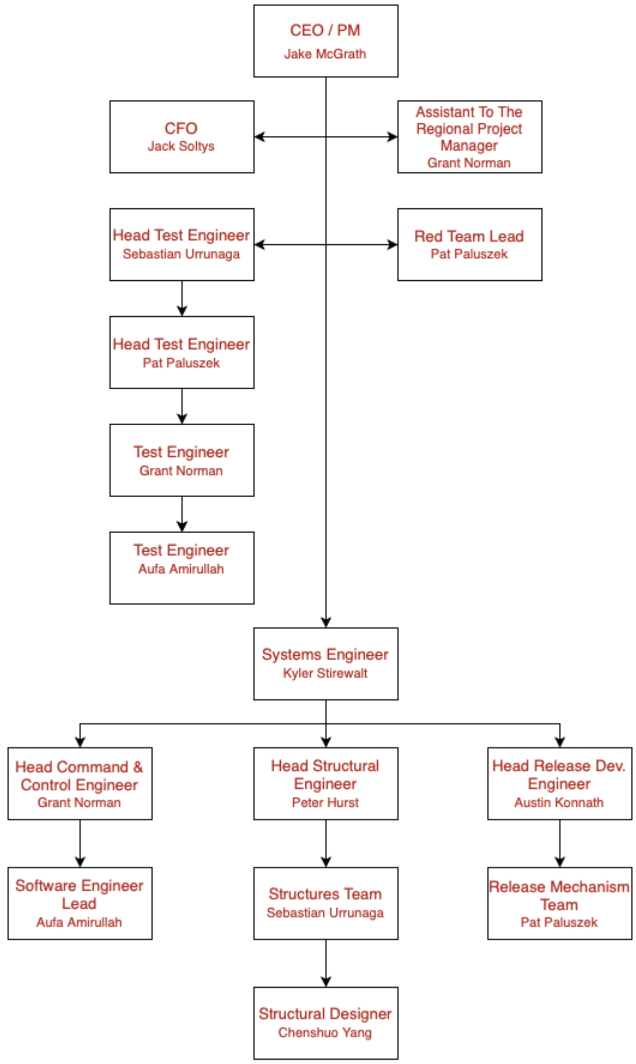

Figure 62 BDS Organization Chart

E. Work Breakdown Structure

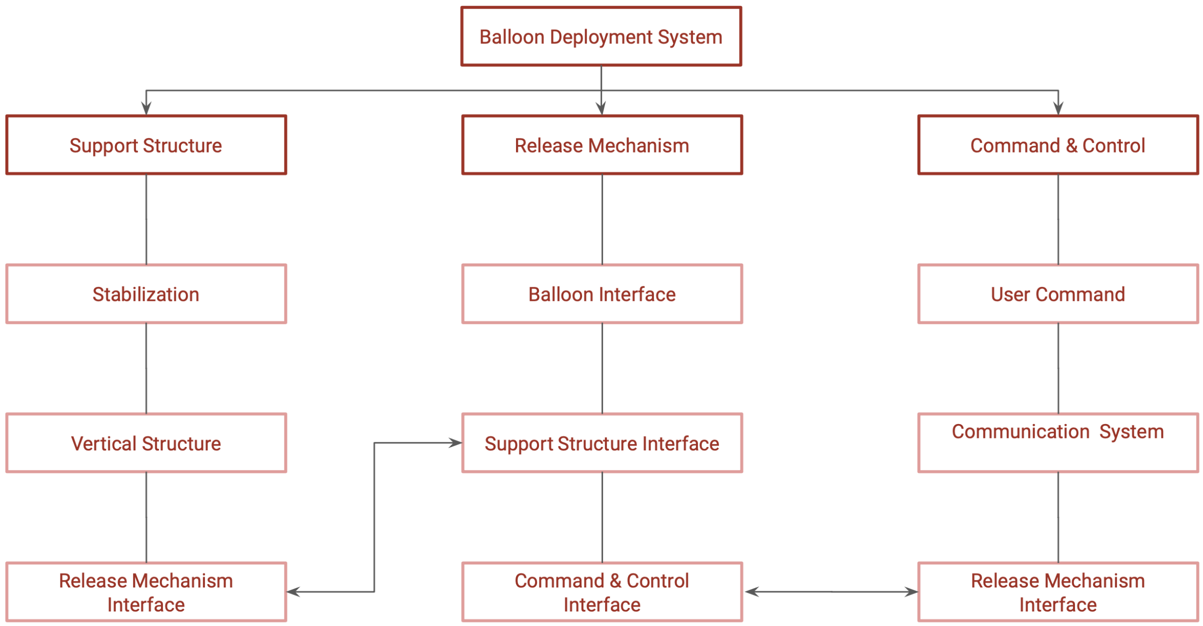

Figure 63 BDS Work Breakdown Structure

References

[1] Taylor, J. R., *An Introduction to Error Analysis*, Sausalito, CA: University Science Books, 1997.
Error Calculations

[2] Kwon, Dae Kun & Kareem, Ahsan. (2014). Revisiting Gust Averaging Time and Gust Effect Factor in ASCE 7. Journal of Structural Engineering. 140. 10.1061/(ASCE)ST.1943-541X.0001102.

[3] https://en.wikipedia.org/wiki/Stiffness. Oct 2020. "Stiffness". Accessed December 7, 2020.

[4] https://www.engineeringtoolbox.com/modulus-rigidity-d_946.html

[5] Shackelford, James F. *Introduction to Materials Science for Engineers.* 8th ed., Pearson Education Limited, 2016.

[6] "ASEN 1022 MTS Tensile Procedure2019 .pdf." Canvas, 2019, canvas.colorado.edu. March 2019. PDF.
Lab Document

[7] MATLAB r2019a, The MathWorks, Inc., Natick, Massachusetts, United States.

[8] "Online Materials Information Resource," MatWeb. Available: http://www.matweb.com/index.aspx.
Materials Data

[9] "ASEN1022_Lab_Description_SS19.pdf." Canvas, 2019, canvas.colorado.edu. March 2019. PDF.
Lab Document

[10] Dugan, S. R., & Komives, J. P. (2010). Political and civic leadership: A reference handbook. Retrieved from https://sk.sagepub.com/reference/civicleadership
Komives and Dugan

[11] Taleb, N. N. (2020). Skin in the game: hidden asymmetries in daily life. Random House.
Skin in the Game